공학석사학위논문

향상된 변조 반송파 제어를 이용한 단상 능동 전력 필터

A Single-phase Active Power Filter with an Improved Modulated Carrier Control

2014 년 2 월

서울대학교 대학원

전기 컴퓨터 공학부

손 기 봉

향상된 변조 반송파 제어를 이용한 단상 능동 전력 필터

A Single-phase Active Power Filter with an Improved Modulated Carrier Control

지도교수 조 보 형

이 논문을 공학석사 학위논문으로 제출함

2014 년 2 월

서울대학교 대학원

전기 컴퓨터 공학부

손 기 봉

손기봉의 공학석사 학위논문을 인준함

2014 년 2 월

위 원 장 : 설 승 기

부위원장 : 조 보 형

위 원 : 하 정 익

Abstract

This thesis proposes a new control method, *improved modulated carrier control*, for single-phase active power filter which eliminates harmonic and reactive currents at ac sources drawn by nonlinear loads.

The new control method directly shapes line current to be sinusoidal and in phase with grid voltage by comparing a modulated carrier signal to the average line current and making duty ratio doubled. Since the line current value compared to the carrier signal is not the peak, but the average, dc-offset problem observed in a similar type of control method is effectively enhanced. The proposed control technique extirpates the harmonic and reactive currents properly and solves the dc-offset problem.

The operation of a shunt active power filter with the proposed control method is discussed and design guideline is given in detail. Experimental results on the basis of laboratory prototype hardware verify its performance.

Keywords: Nonlinear loads, Shunt active power filter, Harmonic and reactive current compensation, Improved modulated Carrier Control.

Student ID : 2012-20794

Contents

List of Tables

List of Figures

1. Introduction

1.1. Thesis Background and Objectives

Recently, usage of nonlinear loads such as diode rectifiers with a capacitive and inductive load has soared. These loads generate a large amount of harmonic and reactive currents from ac sources as shown in Fig. 1.1 and cause low efficiency, low power factor, high total harmonic distortion (THD), and some detrimental disturbances to other devices [1]. Due to the problems, power quality has become a very important research topic and a lot of tight regulations (e.g. IEC 61000-3-2, IEC 61000-3-12) on harmonic and reactive currents have been established to suppress the serious harmonic contamination caused by proliferation of nonlinear loads. In order to satisfy with the regulations and get rid of the harmonic and reactive currents, many specialists have conducted researches and developed a number of solutions along with the remarkable development in power electronics.

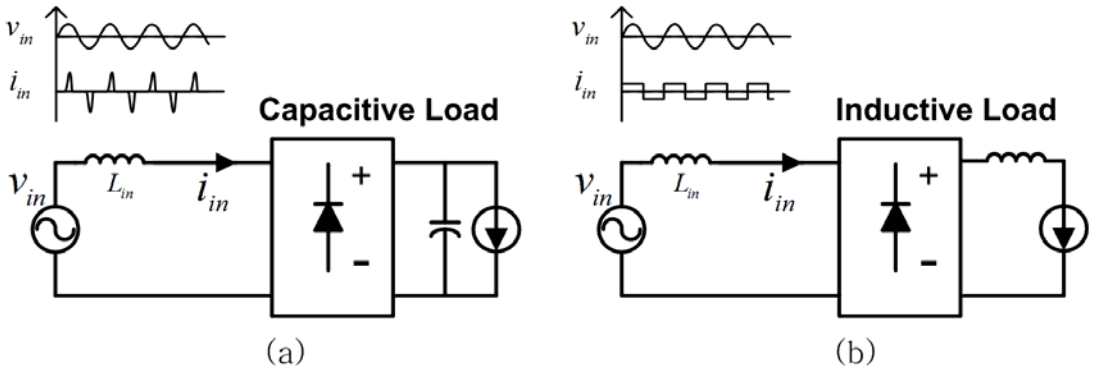

Fig. 1.1 Nonlinear loads: (a) capacitive load (b) inductive load.

For a long time, active power filter (APF) has been considered as a reasonable remedy to tackle the aforementioned issues [2], [3]. Among a variety of APFs, shunt active power filter is one of the most practical configurations because of its simplicity, effectiveness and versatility [4]. Shunt APF is connected in parallel with nonlinear loads and compensates the harmonic and reactive components by working as a current source. Generally, topology of the single-phase shunt APF has been fixed as full-bridge boost converter, thus the most of the researches concerning the single-phase APF system is how to control the shunt APF in a smart way. In this thesis, a new control method of the single-phase shunt APF is mainly treated.

In conventional control method for single-phase shunt APF [5]-[8] known as direct control, in order to obtain a reference current for a control converter, the shunt APF, it is essential to detect the harmonic and reactive elements of the nonlinear load which requires precise analog multipliers or high performance processor and A/D modules. On top of that, these methods not only need two current sensors for both the line current and the control converter current, but also suffer from calculation burden coming from the harmonic detection.

To overcome these shortcomings, indirect control methods have been introduced [9]-[18], which simply control the line current to follow the grid voltage. These methods achieve good harmonic and reactive current elimination at the grid with only one current sensor for the line current and greatly simplify the control circuit because the harmonic detection process is

no longer necessary. However, the approaches based on reference generation method [9]-[14] still require multipliers to scale the fundamental element of the line current according to the load variation. One-cycle based indirect control methods [15]-[18] do not have the disadvantage and furnish the most uncomplicated control circuit. In spite of the merits, dc-offset problem arises which worsens power factor and efficiency because the peak value of the line current is set to be compared to the reference signal.

The objective of this thesis is to propose a new single-phase shunt APF control method using an improved modulated carrier signal and an on-time doubler to solve the dc-offset problem. By comparing the carrier signal to the average line current, the proposed control strategy accomplishes no dc-offset and good current compensation performance.

1.2. Thesis Overview

The thesis includes the following four chapters.

Chapter 2 reviews widely used harmonic and reactive current elimination techniques which are passive filter, active power factor correction, and active power filter. Configurations and main characteristics of each technique are briefly explained.

Chapter 3 first discusses about conventional control strategies of single-phase shunt active power filter, and merits and demerits of the strategies are organized in general. Then, the proposed control method of single-phase shunt APF is introduced with the ensuing sequence: motivation, operation principle, control scheme, voltage controller design, comparison with the conventional control and design procedure.

In chapter 4, simulation and experimental results with a laboratory prototype are provided to validate the performance of the proposed control method.

Finally, conclusion and future work are given in chapter 5.

2. Harmonic and Reactive Current Elimination Techniques

2.1 Introduction

In chapter 2, widely used harmonic and reactive current elimination techniques are reviewed. At the earlier stage, simple passive filter was employed to improve power factor and selectively compensate harmonic currents [20], [35]. Passive filter consists of, as its name implies, sorely passive elements such as inductors, capacitors, and resistors as shown in Fig. 2.1. Basic configurations and characteristics of passive filter are given in 2.2.1.

Another technique is active power factor correction (PFC) which builds an ideal rectifier presenting an effective resistive load to the grid [21]. Therefore, if the grid voltage is sinusoidal, the line current is also sinusoidal and in phase with the grid voltage meaning that a unity power factor is achieved. Amongst various topologies, boost converter is the most typical as the power stage of PFC replacing the diode rectifier of nonlinear loads. Operation principle and constituents of the overall circuit on the basis of a boost converter are described in 2.2.2.

The other technique is active power filter (APF) which is connected in parallel or series with nonlinear loads [22]. Mostly the first one is for current harmonic compensation and the latter is for voltage harmonic compensation. Thus only the former, called a shunt active power filter, is focused in this

thesis, because the new control method proposed in the thesis aims at the line current compensation. The main function of the shunt APF is to supply harmonic and reactive components drawn by the nonlinear load so that the line current includes only the fundamental part of the load current. This technique fulfills excellent current compensation and has many advantages. In addition, APF can be combined with the passive filter, called hybrid active power filter, to enhance its performance and supplement more functions. Hybrid APF is concisely mentioned as well.

2.2 Harmonic Current Elimination

2.2.1 Passive Filters

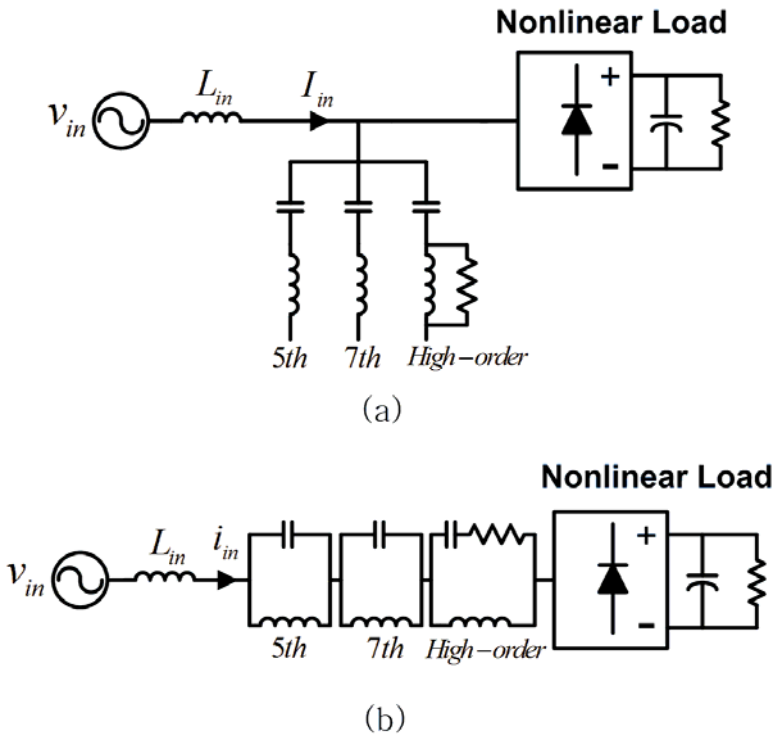

Fig. 2.1 Passive filters: (a) parallel passive filter (b) series passive filter.

Fig. 2.1(a) depicts a passive filter connected in parallel with a nonlinear load. It uses series resonant LC filters and provides low- impedance at 5^{th}, 7^{th}, and high order frequencies of the grid. Since each part of parallel passive filter is tuned at a specific frequency which harmonic current exists at, the harmonic currents flow into the passive filter. In other words, the parallel passive filter behaves as a current sink. Ultimately, the parallel passive filter is a capacitor.

On the other hand, series passive filter shown in Fig. 2.1(b) behaves as a current dam while being placed between the grid and the nonlinear load. It uses parallel resonant LC filters and provides high-impedance at 5^{th}, 7^{th}, and high order frequencies. The series passive filter blocks the harmonic currents at tuned frequencies and is an inductor ultimately.

The resonant frequencies of LC filters, $w_{resonant}$, in both passive filters are derived as (2.1)

$$w_{resonant} = \frac{1}{\sqrt{LC}}. \tag{2.1}$$

This kind of filter features simplicity and inexpensiveness. Due to the merits, it has been extensively utilized, but there are several demerits. Generally, it is bulky in size and heavy in weight. Not only that, passive filter is extremely intolerant of load and line variations. For instance, when it is installed at the grid having different line impedances, resonance between the passive filter and the line impedance may occur resulting in adverse line condition with substantial distortions. Also it is unable to deal with varying harmonic current element and has fixed compensation characteristics. On account of the weakness, diverse techniques have been studied to supplant passive filter and these techniques are described in the following sections.

2.2.2 Active Power Factor Correction

Active power factor correction (PFC) realizes an ideal rectifier that gives an effective resistive load from the view point of ac power line. This suggests

the grid voltage and the line current have the same shapes and be in phase with each other [20]. The ideal rectifier can be implemented by controlling high frequency pulse width modulation (PWM) dc-dc converters, typically boost converter.

The ideal rectifier equivalent circuit model is represented in Fig. 2.2. As expected, the relationship between the grid voltage and the line current is expressed as

$$\frac{v_{in}}{i_{in}} = R_e, \tag{2.2}$$

where R_e is the emulated resistance. The line current is controlled to pursue the grid voltage such that the rectifier presents a resistive load to the ac system. The average power absorbed by the emulated resistance is delivered to the load and expressed as (2.3).

$$P_{avg} = \frac{V_{in,peak}^{\ 2}}{2R_e} \tag{2.3}$$

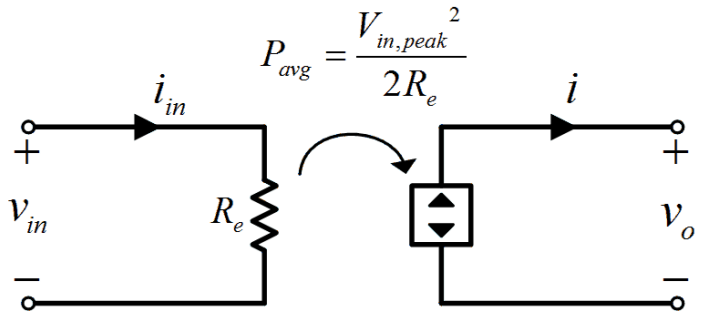

Fig. 2.2 Ideal rectifier equivalent circuit model.

Fig. 2.3 shows power factor correction circuit based on a boost converter. This contains three major power processing parts: a wide bandwidth input current controller, a low bandwidth output voltage controller, and a dc-dc converter, a boost converter in this case.

The grid voltage v_{in} is rectified by the bridge diode. The rectified voltage v_g is multiplied by the control voltage v_c, the output of the voltage controller, to generate the current reference i_g^*. Then, the current controller has the line current trace the current reference.

The current controller can be realized by various control schemes [23]-[26]. Among the current control schemes, the average current mode control [24] is the most widely employed.

Fig. 2.4 illustrates the current and the voltage controllers explicitly. In Fig. 2.4 (a), the error between the current reference and the inductor current i_g is fed to the current controller which modifies the duty by comparing the

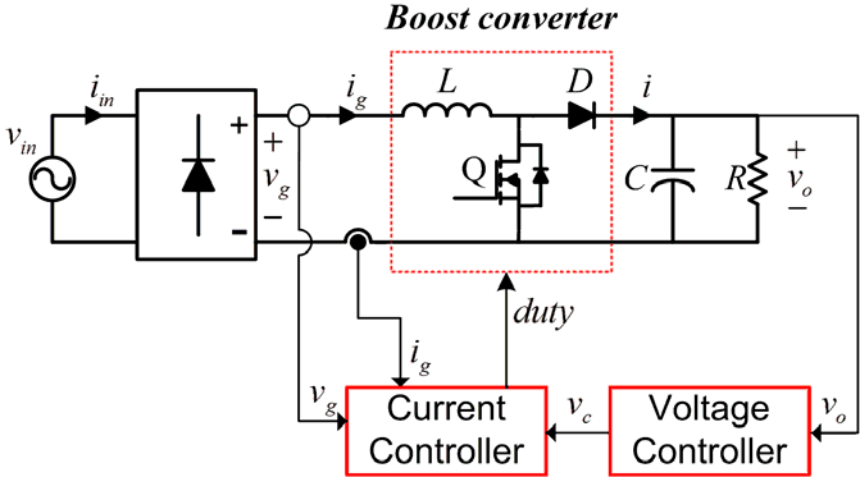

Fig. 2.3 Power factor correction circuit based on boost converter.

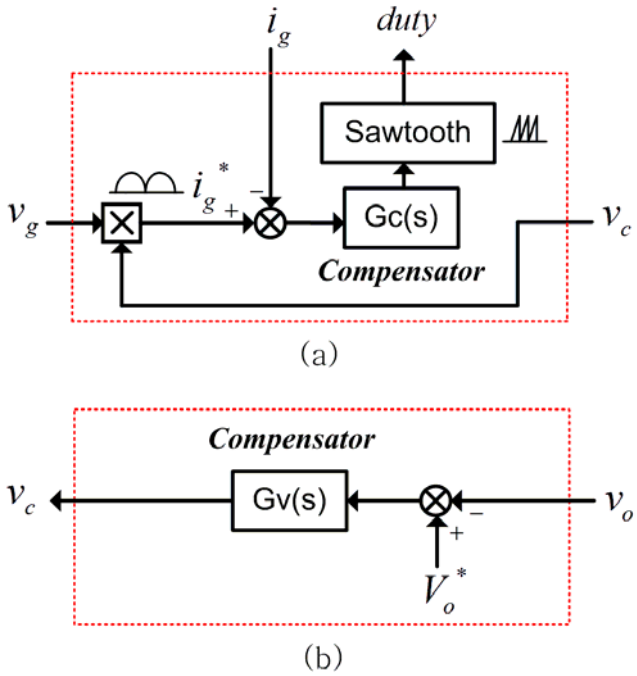

Fig. 2.4 Block diagrams of PFC controllers: (a) current controller (b) voltage controller.

compensator output to a sawtooth signal to force the inductor current to follow its reference.

The current compensator $G_c(s)$ must be designed to have a wide bandwidth for fast current tracking, and, in average current mode control, is given by

$$G_c(s) = w_{ik} \frac{(1+\frac{s}{w_{iz}})}{s(1+\frac{s}{w_{ip}})} \quad . \tag{2.4}$$

Equation (2.4) consists of an integrator, one pole, and one zero. The integrator plays a role to remove DC error, while the zero prevents the slope of current loop from becoming -40dB/decade at crossover frequency to

secure sufficient phase margin. Lastly, the pole acts as a low pass filter to attenuate the high frequency noise.

As for the voltage regulation, the voltage controller must be designed to have a very low bandwidth such as one-fifth (approximately 10Hz) of the line frequency. Increase in the bandwidth of the voltage loop can cause serious line current distortion [27]. R_e varies rapidly leading to the distorted line current waveform, if the control loop has a high gain and a wide bandwidth. The voltage controller is expressed as

$$G_v(s) = w_{vk} \frac{(1 + \frac{s}{w_{vz}})}{s(1 + \frac{s}{w_{vp}})} \quad . \tag{2.5}$$

It is noted from (2.5) that formation and function of the voltage controller are the same as those of the current controller except that the bandwidth of the voltage loop is much lower than that of the current loop. In order to design each part of the controller, small-signal analysis is required. Derivation of voltage loop small-signal modeling is elucidated in [28] in depth.

By controlling a PWM dc-dc converter with the controllers, active power factor correction almost perfectly achieves a unity power factor.

2.2.3 Active Power Filters

Although active PFC performs precise unity power factor, it requires higher rating power semiconductor devices such as MOSFET, and diode because it processes the whole power delivered from the grid to the load. Besides, existing diode rectifiers are replaced by dc-dc converters for active PFC. In this sense, active power filter (APF) is a rational solution in that it retains existing systems and handles only harmonic and reactive components instead of the whole power. It results in efficiency improvement and needs for lower quality active elements than PFC.

Universally, active power filter is classified into three groups, even though it has tons of offspring [29]: 1) Shunt active power filter, 2) Series active power filter, 3) Hybrid active power filter. Shunt APF is aimed at harmonic and reactive current compensation. On the other hand, series APF solves harmonic voltage problems, while hybrid APF furnishes both functions. Since the main target of this thesis is harmonic and reactive current compensation, the explanation about the series APF is omitted.

Fig. 2.5 shows (a) configuration of a shunt active power filter and (b) waveforms of the line current, the load current, and the APF current, respectively. Shunt APF is connected in parallel with the nonlinear load and compensates the harmonic and reactive components by working as a current source so that the net current drawn from the ac source is the fundamental element of the nonlinear load current. Control methods for shunt APF, which

are the most crucial subjects of the thesis, are comprehensively discussed in the next chapter.

Hybrid active power filter is represented in Fig. 2.6. In fact, there are two types of hybrid APFs: 1) shunt APF based HAPF 2) series APF based HAPF [29], yet only the former is covered in this section. Basically, series or parallel passive filter mentioned in 2.2.1 is added to a shunt APF. Depending on which node the passive filter is connected at, two combinations are

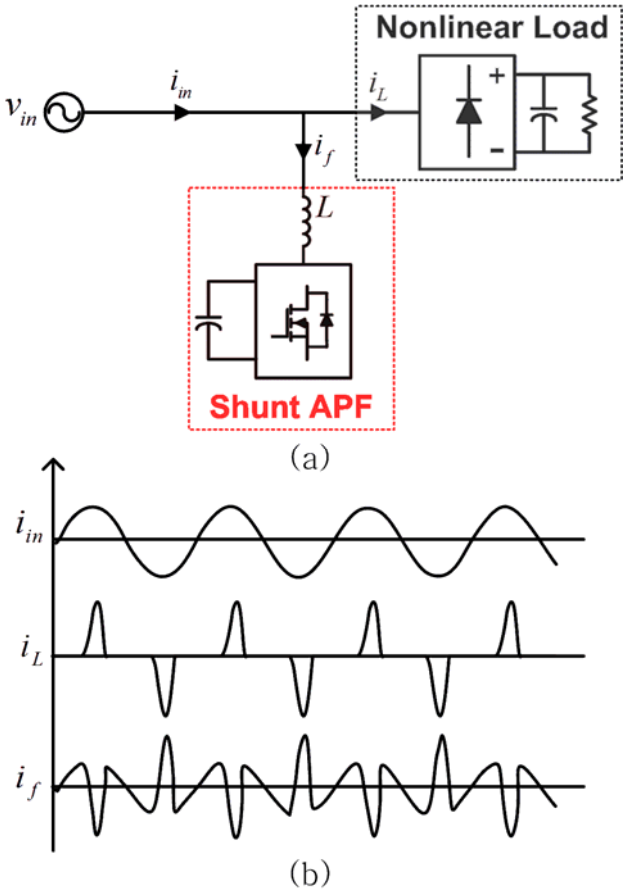

Fig. 2.5 Shunt active power filter: (a) configuration (b) current waveforms.

available. However, the main characteristics are nearly similar that the amount of power handled by APF is greatly reduced compare to the case only shunt APF is used because passive part of the hybrid APF absorbs (parallel passive filter) or blocks (series passive filter) the selected harmonic currents. It is beneficial that the total amount of harmonic currents processed by the shunt APF is substantially reduced, thus design flexibility of the shunt APF increases.

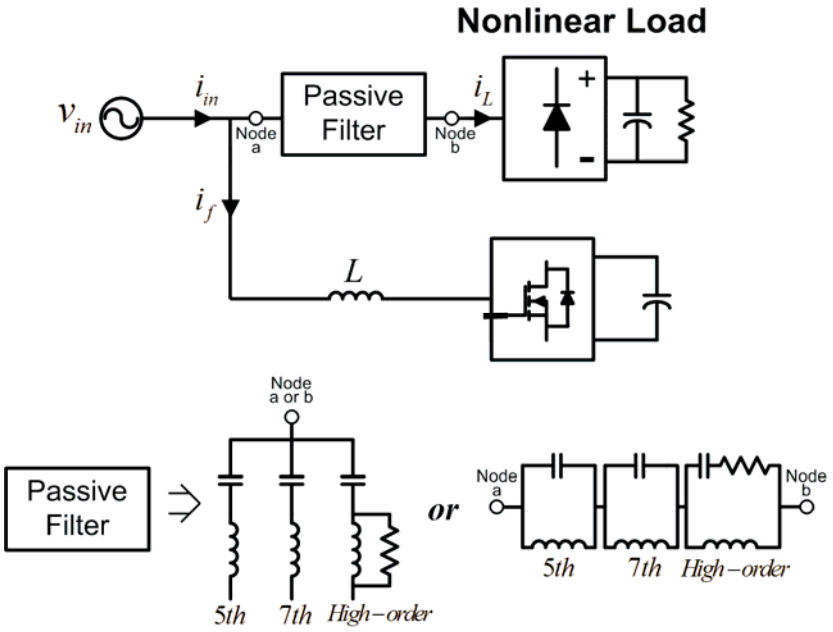

Fig. 2.6 Hybrid active power filter.

2.3 Summary

As aforementioned, several types of harmonic and reactive current elimination techniques are reviewed concisely.

To sum up, passive filters are simple and inexpensive, but bulky, heavy and may cause some complications such as serious distortion by resonance. Active power factor correction achieves unity power factor with high frequency switching converter. Though its performance is outstanding, as PFC circuit deals with the whole power delivered to the load, high quality active components are needed. On the other hand, active power filter is advantageous in that it can be easily exploited in the existing system and only deals with harmonic and reactive elements of the nonlinear load.

3. Single-phase Shunt Active Power Filter

3.1 Introduction

In this chapter, a variety of control methods of single-phase shunt active filter, which is mentioned in 2.2.3, are presented in depth. These methods are categorized into two groups: 1) Direct control method, 2) Indirect control method. Direct control method detects harmonic and reactive elements of the nonlinear load and generates reference current signal for the control converter (shunt APF). Shunt APF is controlled for its current to track the reference signal. The second method directly shapes the line current to be sinusoidal and be in phase with the grid voltage instead of generating the reference current signal for the control converter.

Subsequent to the explanation of conventional control methods, proposed single-phase shunt APF with an improved modulated carrier control is introduced. This control method uses an improved modulated carrier signal and an on-time doubler to overcome limitations the conventional ones connote. By comparing the carrier signal to the average line current, the proposed control technique performs no dc-offset and good current compensation. The operation mode of the power stage is analyzed and whether the proposed control scheme makes sense is evaluated theoretically and mathematically. Then, design guideline of a shunt APF for a particular application is specified after comparison between conventional and proposed control method.

3.2 Conventional Single-phase Shunt Active Power Filter Control Methods

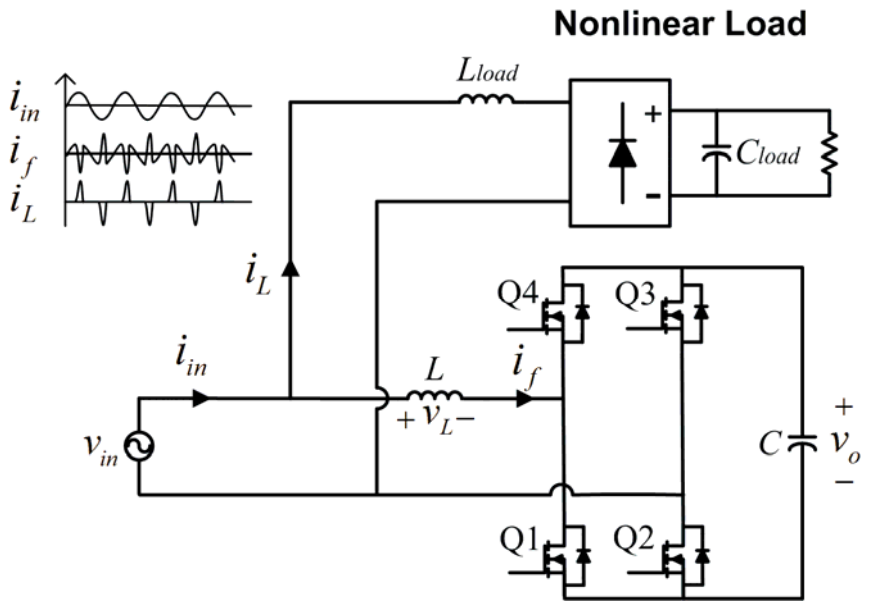

Fig. 3.1 Basic configuration of single-phase shunt APF system.

Fig. 3.1 shows the basic structure of a single-phase SAPF system. It consists of a nonlinear load and a boost type full-bridge converter which operates as the shunt APF. The main purpose of the shunt APF is to eliminate harmonic and reactive currents at ac sources drawn by the nonlinear load so that the line current contains only the fundamental content of the load current. According to which current is controlled, conventional shunt APF control methods are classified into two types.

1) Direct control method

2) Indirect control method

3.2.1 Direct Control Method

The primary feature of this control strategy is detecting the harmonic and reactive component drawn by the load. Fig. 3.2 shows a typical diagram of a shunt APF with the control strategy. The grid voltage and the load current are sensed to figure out how much harmonic and reactive currents flow into the load. Once the unwanted currents are detected, it becomes the reference of the inner current controller. The shunt APF current is subtracted from the reference current signal, and the error is processed through the inner current controller to produce an output signal identical to its reference. To force the inner current to follow the reference, an additional current sensor is required at the path of the inner current.

The key point of the strategy is how to detect the harmonic and reactive elements of the nonlinear load which are designated to be the reference current signal of the shunt APF. For a long time, researches on harmonic detection method have been widely conducted [5]-[8].

In [5], the real part of the fundamental load current is calculated by using two multipliers and an integrator. Difference between the calculated current and the load current becomes the reference current signal of the inner current loop. For reduction in calculation complexity of that proposed in [5], [6] uses the integration and sampling technique to gain the real part of the fundamental load current. On top of that, adapting energy balance concept allows the dc-link voltage control circuit to be simplified. The least compensation technique developed in [7] produces the reference current

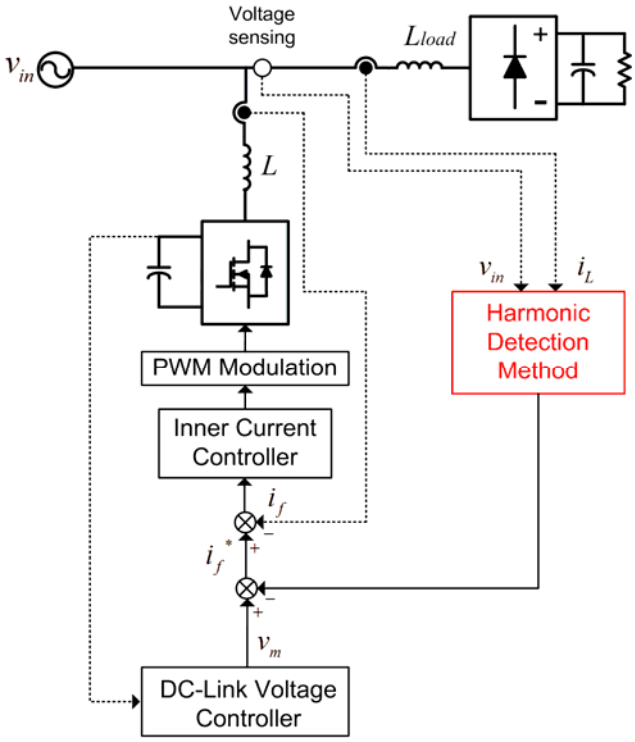

Fig. 3.2 Diagram of a shunt APF with direct control.

signal by detecting the harmonic and reactive currents of not the load current, but the APF current. [8] introduces globally stable control based on Lyapunov's stability theory. This method achieves accurate harmonic detection and better system stability with Lyapunov function.

All of these methods properly compensate the harmonic and reactive currents, but they have several drawbacks. In order to obtain the reference current signal (harmonic and reactive current of the nonlinear load) for the APF current, it is necessary to sense both the load and shunt APF currents. In addition, they require precise analog multipliers or high performance processor and A/D modules for the successful detection.

3.2.2 Indirect Control Method

In contrast to the direct control method, indirect control method simply controls the line current to follow the grid voltage and fulfills good harmonic and reactive current elimination [9]-[18]. The main advantages of this approach are that only one current sensor for the line current is required which greatly simplifies circuit complexity, and faster transient response is attained [12].

In this section, two representative indirect control techniques are explained. The first technique generates the line current reference signal instead of the shunt APF current reference by multiplying the grid voltage and an output signal of the dc-link voltage controller. Then, the shunt APF operates to drive the line current to pursue the grid voltage. On the other hand, the second technique applies one-cycle control [30] to the shunt APF. It employs a resettable integrator as its core component to control the pulse width of the shunt APF so that its current draws exactly opposite to the reactive and harmonic currents made by the nonlinear load.

3.2.2.1 Basic, repetitive, and selective Control

Fig. 3.3 represents a diagram of a shunt APF with basic, repetitive, and selective indirect control which generates a line current reference, not the APF current reference. It contains an outer voltage loop, a reference generator, and an inner current loop. The dc-link voltage is regulated by the outer voltage controller, and the output signal of the controller, v_m, is fed into

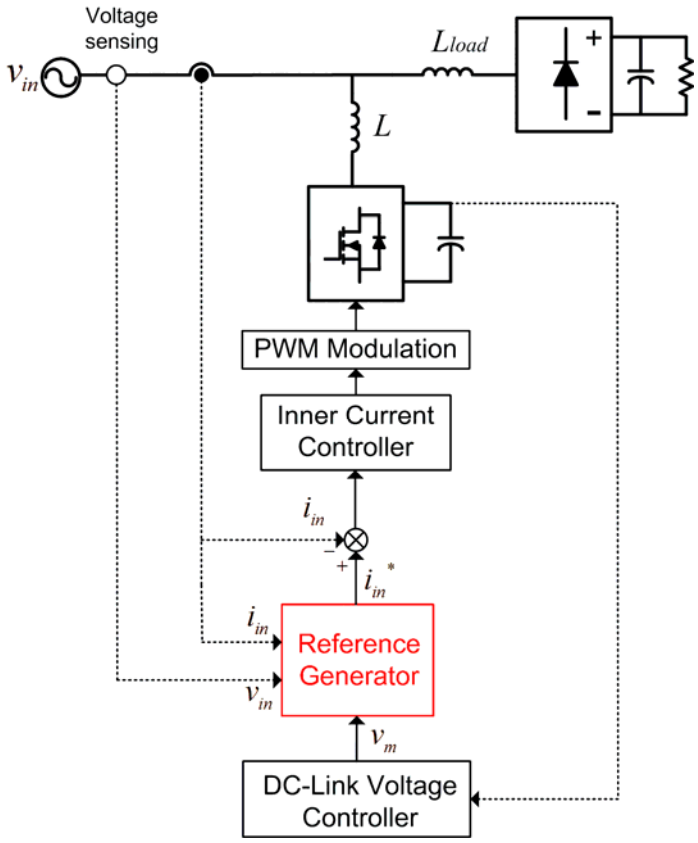

Fig. 3.3 Diagram of a shunt APF with indirect control: basic, repetitive, and selective control.

the reference generator. The inner loop is in charge of reference current tracking. After the sensed line current is subtracted from the reference, the inner current loop copes with the error signal.

The main part of this control method is the reference generator. This section reviews three different types of reference generator [9], [13], [14]. Design of both the dc-link voltage and inner current controller, which are normally PI compensators to ensure stability and low tracking error, is almost

the same in these literatures. The only difference between them is how to realize and implement the line current reference i_{in}^{*}.

Fig. 3.4 illustrates specific means of gaining i_{in}^{*}. Basic approach [5] simply obtains the line current reference by multiplying v_m by the sensed grid voltage [Fig. 3.4(a)] derived as (3.1).

$$i_{in}^{*} = v_m \cdot v_s \tag{3.1}$$

It is noteworthy mentioning that from (3.1) the reference has the same shape of the grid voltage and is in phase. If the grid voltage is perfectly sinusoidal, the line current reference is ideal. However, when the grid voltage is distorted, the shape of the current reference is also distorted causing the increased line current distortion. To raise the quality of the distorted line current in this case, a phase-locked loop (PLL) is needed, but using a PLL augments calculation burden of the controller. Also, the basic indirect control compensates harmonic and reactive currents not completely, but to a certain level. Further elimination of harmonic and reactive currents could trap the system in instability [31].

Repetitive control based approach [13] features better harmonic and reactive current compensation performance, and increased stability. This approach exploits generalized integrators [32] and leading phase delay [Fig. 3.4(b)] to generate the line current reference signal. In order to assure stability that may be deteriorated by significant phase delays at high order harmonics, e^{-NT_s}, which is tuned for leading phase, is used, where N is an

integer and T_s is the sampling time. The generalized integrators in Fig. 3.4(b) are expressed as (3.2) and (3.3).

$$G_1(s) = \frac{2K_{i1}w_c s}{s^2 + 2w_c s + w_1^2} \tag{3.2}$$

$$G_h(s) = \sum_{n=3}^{h} \frac{2K_{ih}w_c s}{s^2 + 2w_c s + w_h^2} \tag{3.3}$$

w_1 is the fundamental frequency of the line current, w_h is the frequency at which harmonic element needs to be attenuated, w_c is the damping term of the generalized integrator, K_{i1} is the gain of the fundamental element, and K_{ik} is the gain of each high order element.

Selective control [14] uses a linear selective harmonic compensator to attenuate further high order harmonic contents in the line current. The function blocks in the control diagram [Fig. 3.4(c)] are almost the same as those in the repetitive approach, but it has slightly different interconnection between them: the line current directly passes through $G_h(s)$, and the outputs of generalized integrators are not summed, but subtracted. This approach provides low sensitivity to both grid voltage distortion and line frequency variation.

However, although these sorts of indirect control have advantages of better transient performance and having only one current sensor, they are still in trouble with calculation burden on reference generation as the load level change and need to use analog multipliers as well.

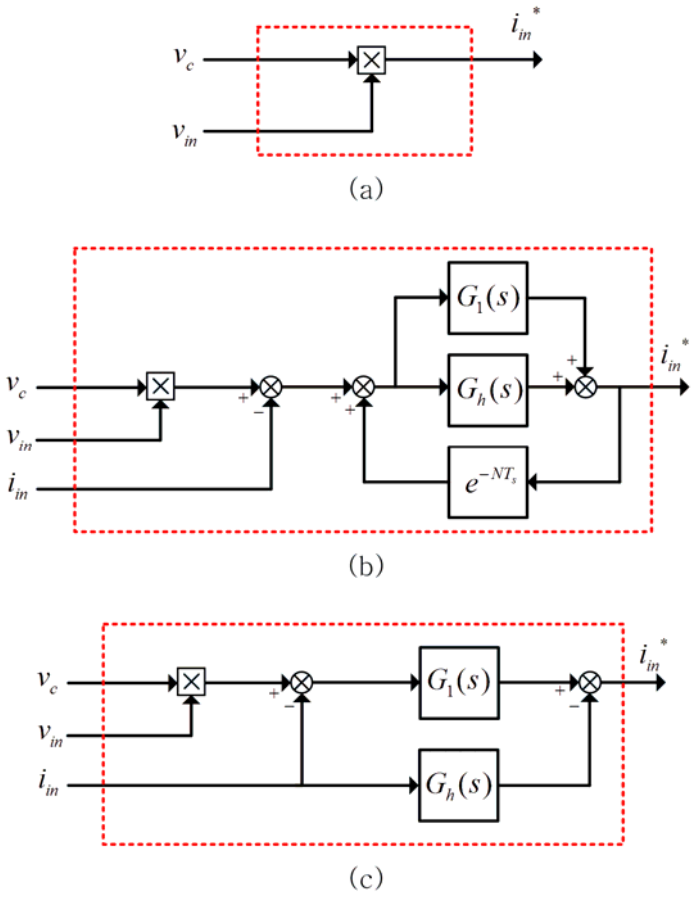

Fig. 3.4 Block diagrams of reference generators: (a) basic control (b) repetitive control (c) selective control.

3.2.2.2 One-cycle Control

In contrast to the indirect control method introduced in 3.2.2.1, the indirect control based on one-cycle control do not need an inner current loop, but uses an integrator with reset as key component to control the duty of APF such that the current flowing through the APF is totally opposite to the harmonic and reactive currents drawn by the nonlinear load [15]. The fundamental

principle of the method called one-cycle control is explained in [30] concretely.

Fig. 3.5 shows the overall diagram of a shunt APF based on one-cycle control. It includes an outer voltage loop, a resettable integrator, and a simple SR latch. It is implied that, compared to other control strategies aforementioned, the control circuit is much less complicated boasting that precise multipliers or high performance DSPs are not required.

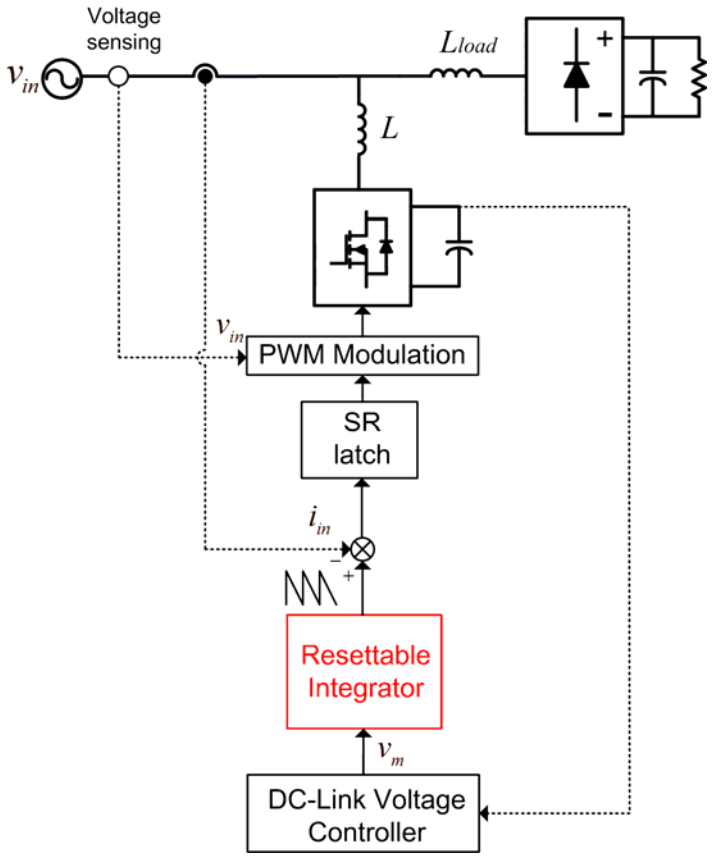

Fig. 3.3 Diagram of a shunt APF with indirect control based on one-cycle control.

In this control method, the power stage of the shunt APF is operated in bipolar mode. In order to shape the line current to trace the grid voltage and to be in phase, the sensed line current must be compared to a carrier signal which is derived as

$$v_c = v_m(1-\frac{2t}{T_s}), \tag{3.4}$$

where v_m is the output of the voltage controller, T_s is the switching period. v_m is obtained from the voltage controller by power balancing technique[27] and determines the peak value of the carrier signal. Then, by the time the sensed line current gets to the carrier signal, the duty of switches is decided. The operation waveforms of the control method are elucidated in Fig. 3.6, where d is the duty ratio, and $R_s i_{in}$ is the sensed line current.

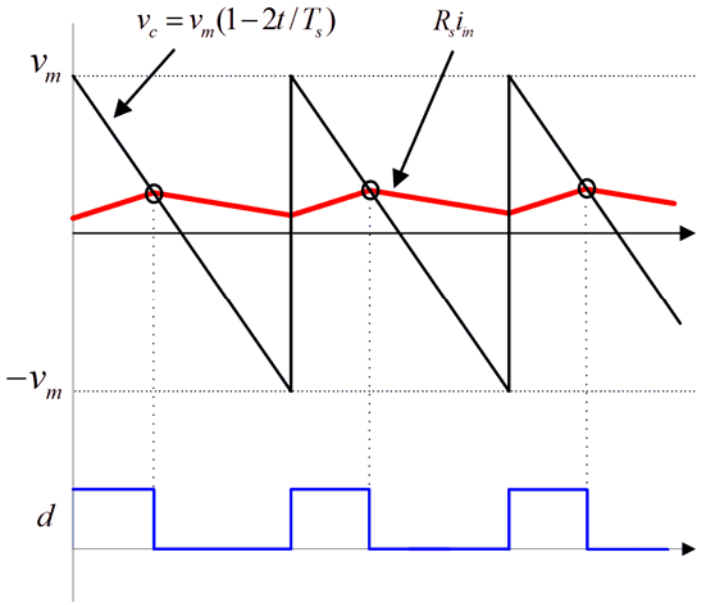

Fig. 3.6 Operation waveforms of a shunt APF based on one-cycle control.

A similar control method using unipolar mode operation was proposed in [17]. Also, the brilliant idea was extended to a three-phase shunt active power system in [18]. In [19], a novel control scheme was proposed to separate harmonic and reactive components and compensate them severally which was impossible in the earlier approaches.

Along with the most simple control circuit, one-cycle control for shunt active filter exhibits good harmonic and reactive current compensation capability. Nevertheless, since the line current value compared to the carrier signal is not average, but peak, dc-offset phenomenon is observed. Several efforts [16], [17] have been made to remove the dc-offset problems, but it is not perfectly addressed.

3.3 Proposed Single-phase Shunt Active Power Filter with an Improved Modulated Carrier Control

3.3.1 Motivation

Amongst multiple control methods for single-phase shunt active power filter overviewed in 3.2, one-cycle based control method is implemented by the simplest control circuit and performs harmonic and reactive current compensation properly. However, as stated before, because the peak value of the line current is programmed to be compared with the reference signal, dc-offset arises especially at light loads. The dc-offset problem deteriorates power factor and efficiency. In this section, a new single-phase shunt APF control method using an improved modulated carrier signal and an on-time doubler to overcome the dc-offset problem is proposed. By comparing the carrier signal to the average line current, the proposed control technique accomplishes no dc-offset and good current compensation performance.

3.3.2 Operation Analysis of Power Stage

Fig. 3.1 shows the power stage of a single-phase shunt APF connected in parallel with a nonlinear load. The shunt APF is operated as voltage-sourced converter and compensates the harmonic and reactive currents, so that the net current drawn from the ac source is the fundamental element of the nonlinear load current.

The shunt APF with the proposed control method is operated in bipolar mode which is illustrated in Fig. 3.7. At positive half cycle of the grid voltage, Q1, Q3 are on and Q2, Q4 are off during $0<t<dT_s$, and Q2, Q4 are on and Q1, Q3 are off during $dT_s<t<T_s$, vice versa at negative half cycle, where T_s is the switching period and d is the duty ratio of the converter.

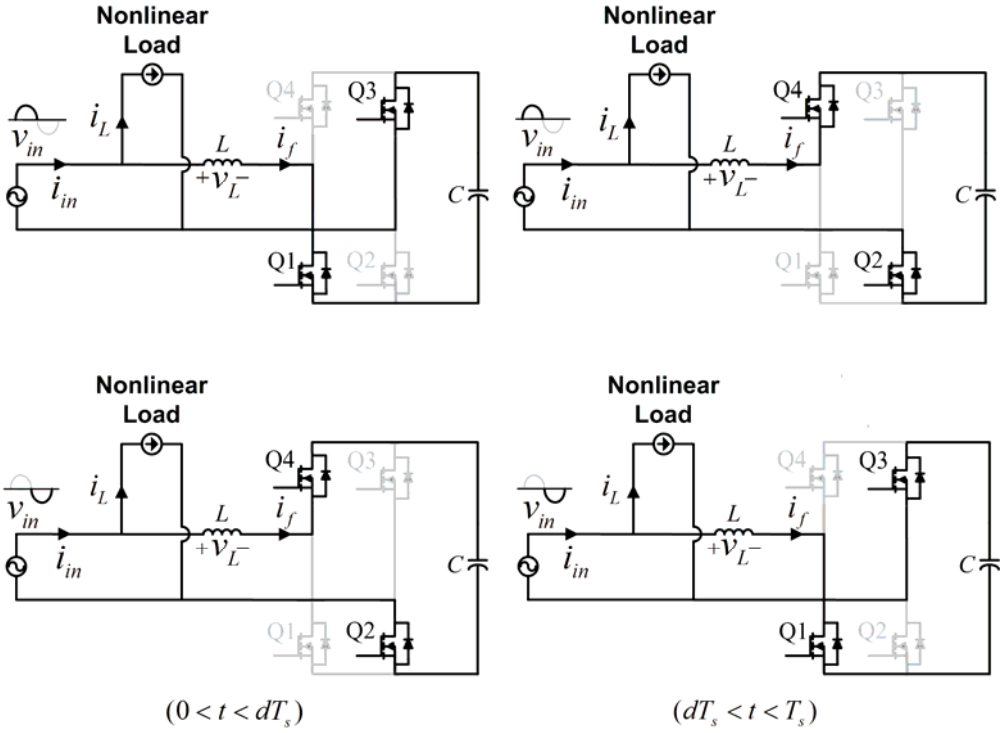

Fig. 3.7 Operation modes of shunt APF power stage.

On the assumption that 1) the switching frequency of the shunt APF f_s is much higher than those of the line and the nonlinear load currents, 2) the capacitance of the dc-link capacitor C is large enough so that v_o is regulated to be a constant value V_o in each switching cycle, the shunt APF current i_f is approximately constant during a switching period.

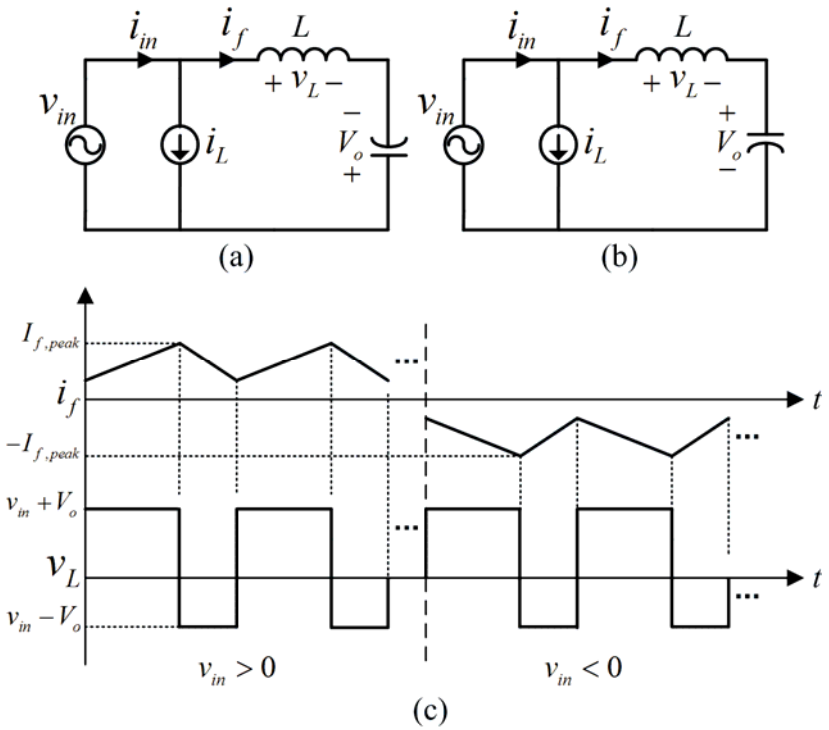

Fig. 3.8 Equivalent circuit of the shunt APF and operation waveforms:
(a) $0<t<dT_s$ (b) $dT_s<t<T_s$ (c) APF inductor current and voltage.

Then, by using voltage-second balance of the APF inductor L in the equivalent circuit of shunt APF shown in Fig.3.8,

$$L\frac{di}{dt} = v_{in} + V_o \quad (0 < t < dT_s), \tag{3.5}$$

$$L\frac{di}{dt} = v_{in} - V_o \quad (dT_s < t < T_s), \tag{3.6}$$

$$d(v_{in} + V_o) + d'(v_{in} - V_o) = 0. \tag{3.7}$$

From (3.5) and (3.6), (3.7) is derived, and the relation between the grid voltage v_{in} and shunt APF's dc-link voltage V_o is given by

$$V_o = \frac{1}{(1-2d)} v_{in} \,. \tag{3.8}$$

3.3.3 Proposed Control Scheme

To make the line current follow the grid voltage, (3.9) must be satisfied that is a key concept of power factor correction (PFC) control.

$$\frac{v_{in}}{\overline{i_{in}}} = R_e \,, \tag{3.9}$$

where $\overline{i_{in}}$ is the averaged line current in one switching period and R_e is the constant of proportionality known as the emulated resistance. By combining (3.8) and (3.9), the control equation for the proposed control method is presented as

$$R_s \overline{i_{in}} = R_s \cdot \frac{V_o}{R_e}(1-2d) = v_m(1-2d) \,, \tag{3.10}$$

where R_s is the line current sensing gain and v_m is $V_o R_s / R_e$. Then, (3.9) is realized by controlling d to satisfy (3.10) in a switching cycle.

Fig. 3.9 illustrates the proposed control circuit with a shunt APF. In Fig. 3.9, the nonlinear load current i_L is represented as a current source. The control circuit consists of a voltage controller, a resettable integrator, a comparator, an on-time doubler, a zero crossing detection circuit and a bidirectional switch for the line current sensing. The sensed dc-link voltage is compared to the reference voltage V_{ref} and the error is fed to the voltage controller. The voltage controller output v_m determines the amplitude of the

carrier signal. The carrier signal, v_c, is generated by integrating v_m with a time constant $\tau=T_s/4$ and substracting it from v_m expressed as (3.11).

$$v_c(t) = v_m(1-\frac{4t}{T_s}) \quad (0 < t < T_s) \tag{3.11}$$

When $R_s i_{in}$ reaches v_c, the comparator outputs d_x and this signal is processed to be doubled $2d_x$ by the on-time doubler [33],[34] in Fig. 3.9.

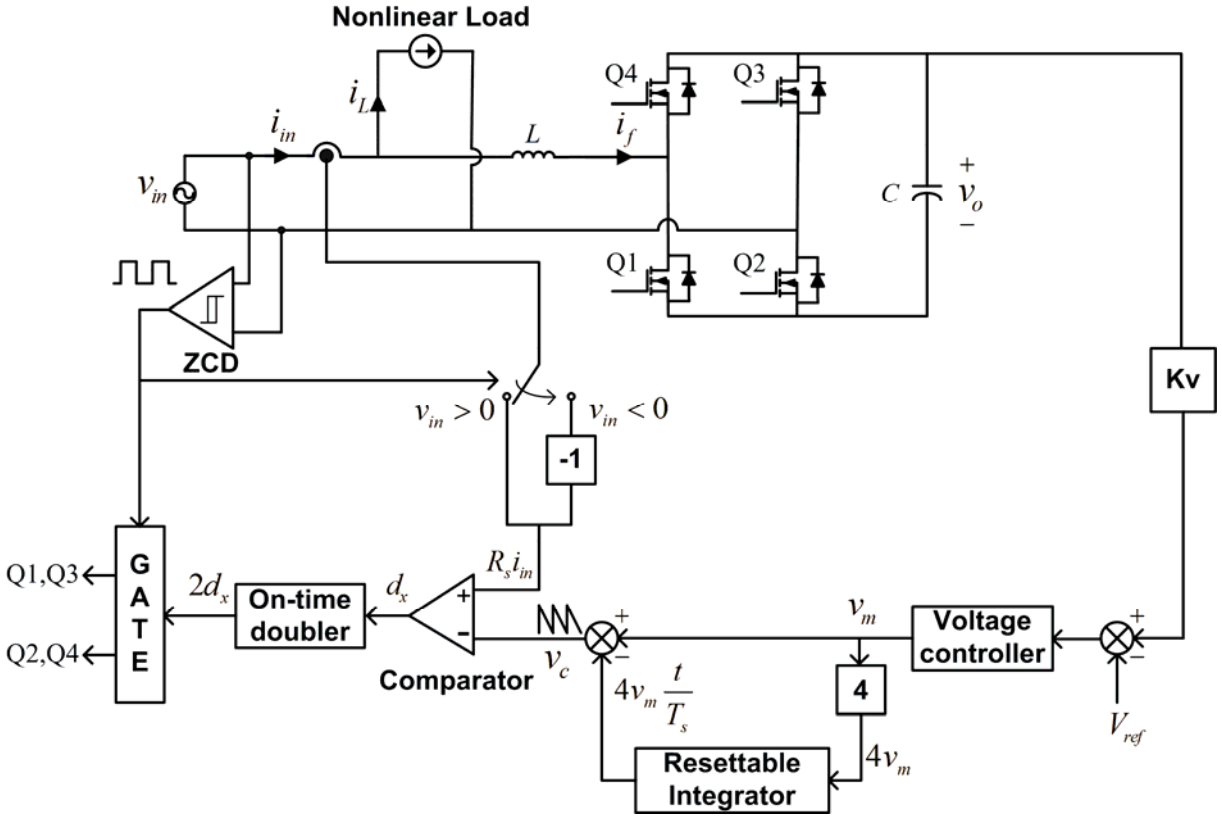

Fig. 3.9 Control circuit of the proposed control method with a shunt APF.

The processed signal d becomes the duty ratio of the shunt APF. Modifying the duty ratio d as the two-fold of d_x allows v_c to be compared with the average value of the sensed line current $R_s\overline{i_{in}}$ which, in turn, guarantees no appearance of the dc-offset problem. Fig. 3.10 shows mechanism of the proposed control method and the following equation is obtained at $t=T_x$.

$$v_x = R_s \cdot \overline{i_{in}} = v_c(T_x) = v_m(1-\frac{4T_x}{T_s}) = v_m(1-2d) \qquad (3.12)$$

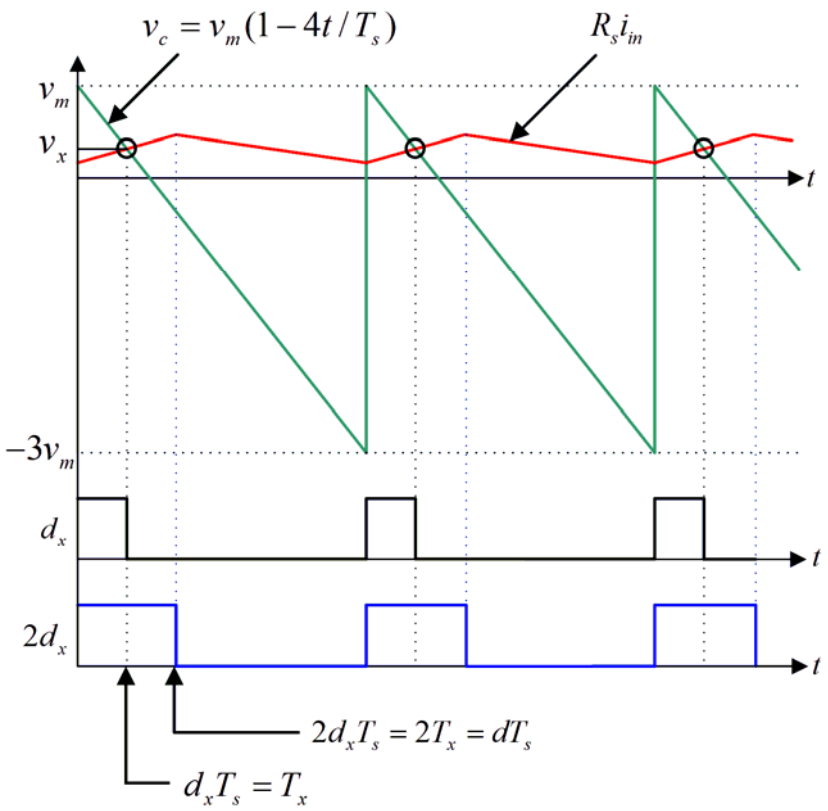

Fig. 3.10 Operation waveforms of the proposed control method.

Combination of (3.8) and (3.12) yields

$$\frac{v_{in}}{i_{in}} = R_s \cdot \frac{V_o}{v_m} = R_e . \tag{3.13}$$

It can be inferred from (3.13) that the average line current is proportional to v_{in} and this allows a unit power factor with the grid voltage. Therefore, parallel connection of the nonlinear load and a shunt APF emulates a resistive load from the viewpoint of the ac source.

3.3.4 DC-link Voltage Control

To regulate the dc-link capacitor voltage, the voltage controller needs to be designed properly. For such design, small-signal transfer function of control voltage v_m to output voltage v_o is clarified. This step starts from the large-signal modeling of the shunt APF system. Power balance technique can derive the large-signal model in a line cycle when assuming that the shunt APF is loss free. The input power is equal to the sum of the output power consumed by the nonlinear load and that handled by the shunt APF [17], that is

$$p_{in} = \frac{v_{in,rms}^{\ 2}}{R_e} = p_{out} = P_{load} + v_o \cdot i_o , \tag{3.14}$$

where p_{in} is the instantaneous input power, p_{out} is the total power consumed by the APF system, P_{load} is the nonlinear load power, and i_o is the dc-link capacitor current. Notionally, the output of the voltage controller is defined as

$$v_m = R_s \cdot \frac{v_o}{R_e} \rightarrow R_e = R_s \cdot \frac{v_o}{v_m}. \tag{3.15}$$

Substituting (3.15) into (3.14) yields the large-signal equation (3.16) that represents the overall power flow of the system as shown in Fig. 3.11.

$$\frac{v_{in}^{\ 2}}{R_s \cdot v_o} \cdot v_m = P_{load} + v_o \cdot i_o. \tag{3.16}$$

To construct the small-signal model, using perturbation and linearization process on (3.16) derives the following equation.

$$\hat{i}_o = g_m \cdot \hat{v}_{in} + j_m \cdot \hat{v}_m - \frac{2I_o}{V_o} \cdot \hat{v}_o, \tag{3.17}$$

where
$$g_m = \frac{2V_{in} \cdot V_m}{R_s \cdot V_o^{\ 2}}, \tag{3.18}$$

and
$$j_m = \frac{V_{in}^{\ 2}}{R_s \cdot V_o^{\ 2}}. \tag{3.19}$$

Since it is assumed that the large-signal model is ideal, the dc value of capacitor current I_o is zero. Then, the small-signal model is simplified as Fig. 3.11 (b). The small-signal transfer function from the capacitor current to the output voltage is expressed as

$$\frac{\hat{v}_o}{\hat{i}_o} = \frac{1}{sC}. \tag{3.20}$$

Finally, the control voltage to output voltage small signal transfer function is yielded by combination of (3.17) and (3.20).

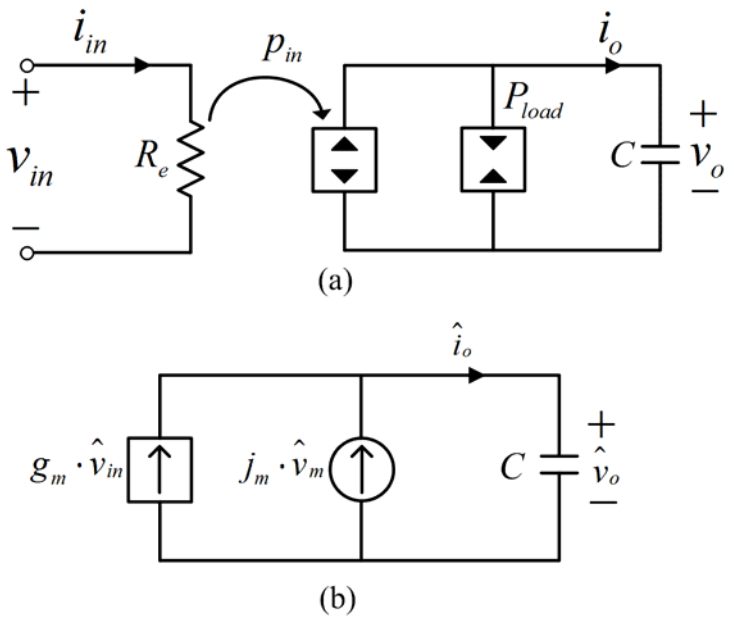

Fig. 3.11 (a) Large-signal low frequency model of the shunt APF system (b) small-signal model of the shunt APF system.

$$\frac{\hat{v}_o}{\hat{v}_m} = j_m \cdot \frac{1}{sC}. \tag{3.21}$$

With the transfer function acquired above, the voltage controller $G(s)$ should be designed advertently based on (3.21).

$$G(s) = w_k \frac{(1+\frac{s}{w_z})}{s(1+\frac{s}{w_p})}. \tag{3.22}$$

As the small signal modeling is done on the average basis over the line cycle which implies that it is a low frequency model, crossover frequency

must be below the line frequency such as 10 Hz. The zero needs to be place at far below the crossover frequency to assure sufficient phase margin. The pole takes on a role to attenuate the high frequency noise, so it is located above the crossover frequency.

If the voltage loop is aptly closed with a well-designed voltage compensator, as the nonlinear load varies, v_m including the information about the nonlinear load changes as well.

3.3.6 Comparison between Conventional and Proposed Methods

Table 3.1 Control scheme comparison

	Conventional	**Proposed**
Carrier Signal	$v_m(1-2t/T_s)$	$\boldsymbol{v_m(1-4t/T_s)}$
Compared Value	v_c & $R_s i_{in,peak}$	$\boldsymbol{v_c}$ **&** $\boldsymbol{R_s i_{in,avg.}}$
Duty	When $v_c=R_s i_{in,peak}$	**When** $\boldsymbol{v_c=R_s i_{in,avg.}}$ **· 2**
DC-offset	Exist	**Not exist**

Table 3.1 arranges comparison between one-cycle based conventional control and the proposed control schemes. The carrier signal slope in the proposed control is two times of that in the conventional control. Also, compared value to the carrier signal is the average line current, and duty becomes twice. By virtue of the control mechanism of the new idea, the shunt APF system inherently does not have dc-offset problem.

3.4 Design Procedure of a Shunt Active Power Filter with the Proposed Control Method

In this section, detailed design procedure of a shunt APF with the proposed control method is guided. The target model of the shunt APF is 1.6 kW home air-conditioner outdoor unit which takes up high portion of power consumption at home. Specification of the shunt APF system is organized in Table. 3.2.

Table 3.2 Specification of the shunt APF
for 1.6-kW home air-conditioner outdoor unit

Maximum Load Power(P_{load})	1.6 kW
APF Current Ripple(Δi_f)	2 A
Grid Voltage(v_{in})	220 Vrms/60 Hz
DC-link Voltage(V_o)	400 ± 2.5%
Switching Frequency(f_s)	60 kHz

3.4.1 Power Stage Parameter Design

To select the value of the APF inductor, the inductor current ripple is considered which is expressed as

$$\Delta i_L = \frac{v_{in} + V_o}{2L \cdot f_s} \cdot d \ . \tag{3.23}$$

Since the dc-link voltage V_o and switching frequency f_s are fixed, the grid voltage v_{in} and duty ratio d decide the current ripple. In consideration of the extreme cases such as $v_{in} = 0$ and $v_{in} = 220\sqrt{2}$, the maximum duty $d_{\max}$ and minimum duty $d_{\min}$ are determined from the equation below.

$$d = \frac{1}{2}(1 - \frac{v_{in}}{V_o}) \tag{3.24}$$

$$\begin{cases} d_{\min} = 0.11 & (\text{when } v_{in} = 0) \\ d_{\max} = 0.5 & (\text{when } v_{in} = 220\sqrt{2}) \end{cases} \tag{3.25}$$

It is inferred that the current ripple is the largest when the grid voltage is zero by putting the values in (3.25) into (3.23). 1 mH inductor is chosen for the current ripple not to exceed 2 A.

When it comes to the dc-link capacitor, the dc-link voltage variation is taken into account [5]. The fluctuating voltage of the dc-link capacitor is represented as

$$\Delta v_o = \frac{1}{C}\int \Delta i_o dt \approx \frac{1}{CV_o}\sum_{n=1}^{\infty}\frac{P_n}{nw}\sin(nwt + \phi_n) \ , \tag{3.26}$$

where i_o is the capacitor current, n is an integer indicating harmonic orders, P_n is the power generated by n[th] harmonic element, and ϕ_n is the phase of n[th] harmonic element. As seen in (3.26), the dc-link voltage variation counts on not only load type, but also APF's power rating. In case precise analysis of load type is not done, capacitance is expected to be sufficiently large for small variation of the dc-link voltage. 800 μF capacitor is selected to restrict the variation to 2.5% of the average dc-link voltage.

3.4.2 Current Loop Implementation

In Fig. 3.9, it is noted that current loop consists of two parts: 1) A resettable integrator, 2) An on-time doubler. The resettable integrator, which generates the modulated carrier signal, is implemented with a conventional integrator and a reset switch as shown in Fig. 3.12.

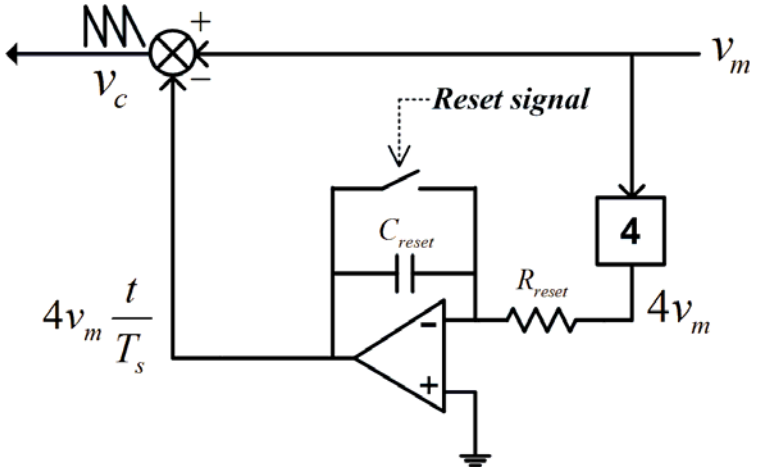

Fig. 3.12 Resettable integrator for the modulated carrier signal.

The frequency of the reset signal is as the same as switching frequency (60 kHz) and originated from a digital signal processor (DSP). To obtain desired signal, R_{reset}, C_{reset} are selected by the integrator frequency derived as

$$w_{reset} = \frac{1}{R_{reset} C_{reset}} . \tag{3.27}$$

After the implementation of the resettable integrator, the sensed line current is compared to the modulated carrier signal created by the resettable integrator. The comparator output is entered into the DSP, then the DSP generates doubled on-time duty depicted in Fig. 3.13. Fig. 3.13 (b) shows how the doubled on-time is generated. Conceptually, it is explained in Fig. 3.10, but, in the practical case, the comparator outputs high signal when the sensed line current reaches the carrier signal, and the output goes into the DSP. During every switching period, an internal counter of the DSP is increasing and detects rising edge of the comparator outputs. At the time the rising edge is detected, the DSP multiplies two by the internal counter value becoming the doubled duty signal.

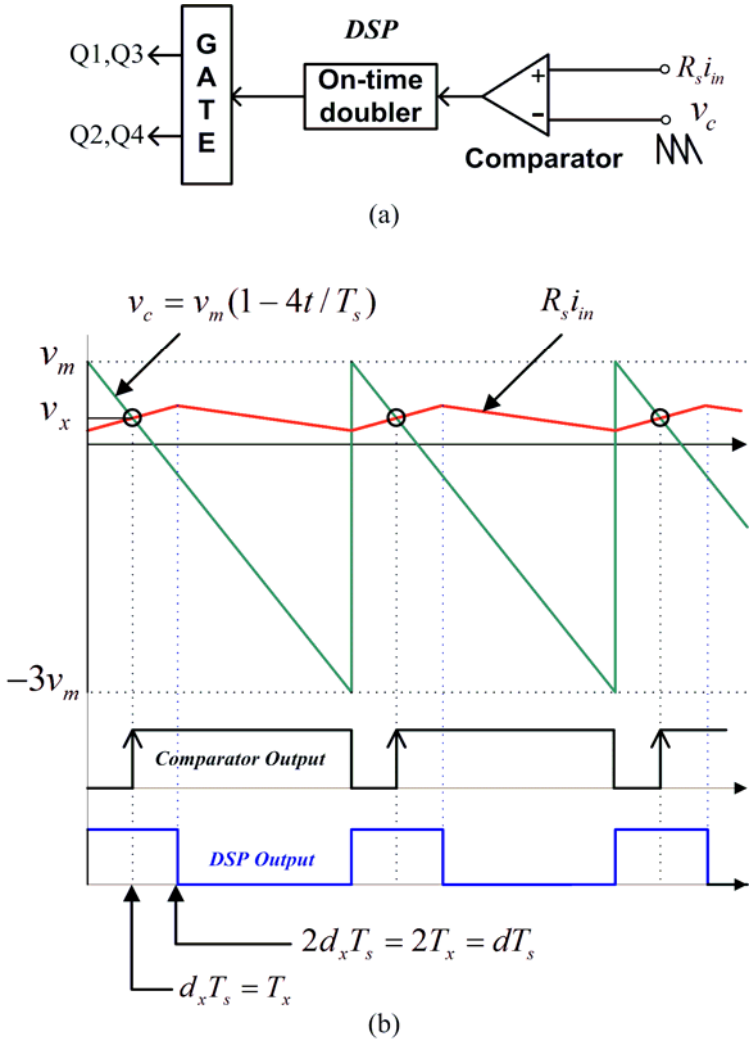

Fig. 3.13 On-time doubler:(a) diagram (b) main waveforms.

3.4.2 Voltage Controller Design

From the equation (3.15) and (3.20), according to different current sensing gain R_s, a bode plot of the voltage loop without compensator is acquired as shown Fig. 3.14.

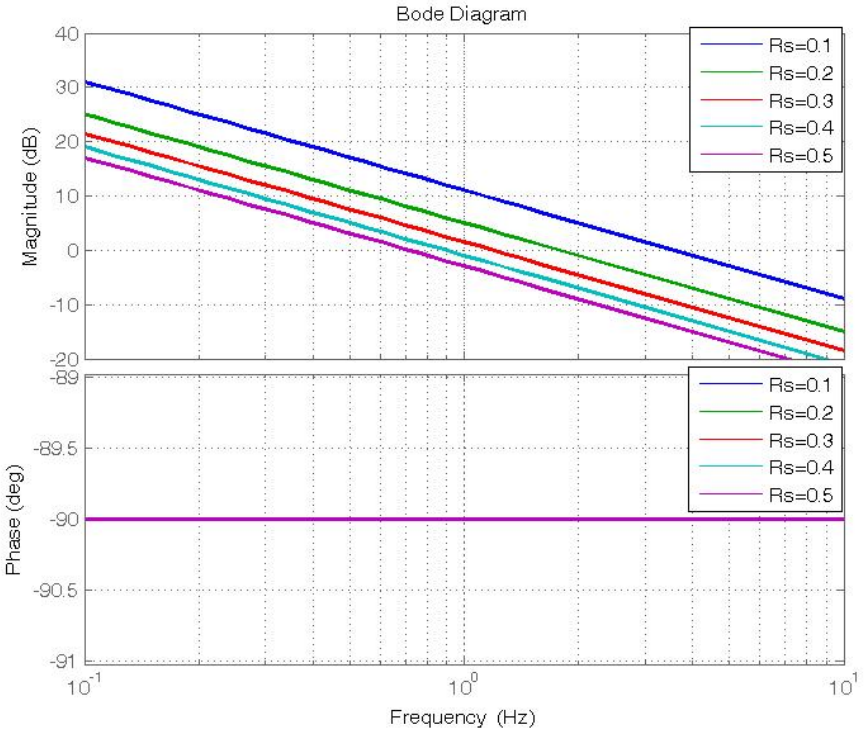

Fig. 3.14 Bode diagram of voltage loop without the voltage controller.

Since the voltage compensator output v_m is expressed as

$$v_m = R_s \cdot \frac{V_o}{R_e} = R_s \cdot \frac{V_o}{V_{in}} \cdot I_{in}, \tag{3.28}$$

if R_s is too large, v_m becomes large as well. It is not recommended to have large v_m, because the voltage compensator, which normally constructed by an OP. AMP., has limited output range clamped by supply voltages. Therefore, in this design procedure, 0.2 ohm is chosen.

In matters of the voltage compensator, the zero is placed at 1 Hz to prevent the slope of the voltage loop from becoming -40dB/decade at crossover frequency ensuring sufficient phase margin, while the pole is placed at 600 Hz to attenuate the high frequency noise, but not to affect phase margin as explained in 3.3.4. With the voltage controller, the bode diagram of the closed voltage loop is plotted as Fig. 3.15. It can be seen in Fig. 3.15 that since the voltage loop has very low bandwidth (10.6 Hz) and sufficient phase margin (77.5 degree), it works stably.

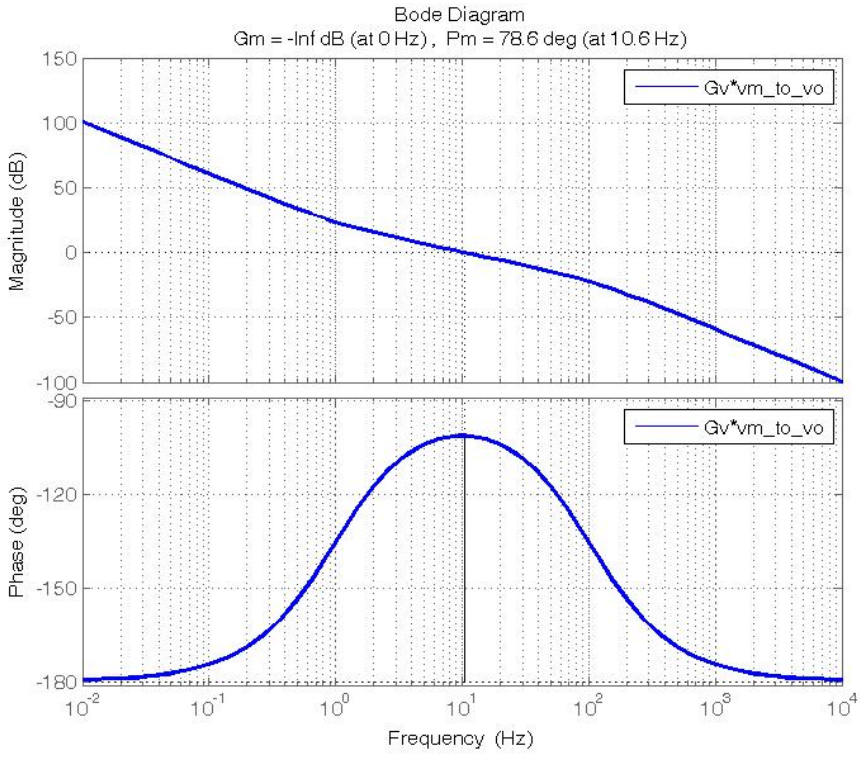

Fig. 3.15 Bode diagram of closed voltage loop with the controller.

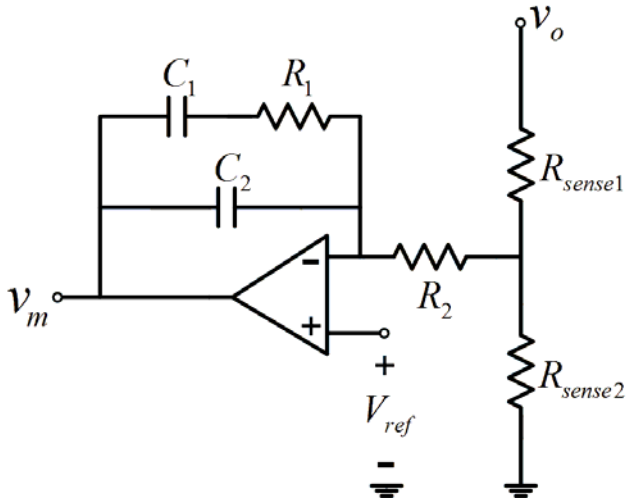

Fig. 3.16 Practical circuit of the voltage controller.

The practical voltage controller is implemented as Fig. 3.16. v_o is sensed and divided by sensing resistors. The sensed value becomes the input signal of the voltage controller. The pole, zero, and controller gain are selected by equations below.

$$K_v = \frac{1}{R_2(C_1 + C_2)} \tag{3.29}$$

$$w_z = \frac{1}{R_1 \cdot C_1} \tag{3.30}$$

$$w_p = \frac{C_1 + C_2}{R_1 \cdot C_1 \cdot C_2} \tag{3.31}$$

Precaution of designing the voltage loop is to prevent dc-link voltage sensing part and controller part from interaction between them that could happen due to improperly designed impedance of each part.

3.5 Summary

In this chapter, conventional single-phase shunt active power filter control methods were analyzed. Direct control method detects the harmonic and reactive currents drawn by nonlinear loads, then controls the APF current to track the unwanted currents. Indirect control method based on the reference generator creates the line current reference and directly controls the APF for the line current to follow the reference. This method has an advantage of sensing only the line current, but is still in trouble with calculation burden on reference generation as the load level changes and need to use the multiplying function, which the direct control method involves as well. Indirect control method based on one-cycle control resolves these obstacles with the most uncomplicated control circuit by using a resettable integrator. However, the dc-offset phenomenon is observed because of the sensed line current value that is compared to the carrier signal.

The proposed control method in this thesis aims at removing the dc-offset problem of the indirect control method based on one-cycle control. Operation principle was analyzed and validity of the proposed control scheme was theoretically proved. In addition, the design guideline for a shunt active power filter with the new control method targeting at a specific application was given.

4. Simulation and Experimental Results

4.1 Introduction

In this chapter, simulation and experimental results are given which validate the performance of the shunt active power filter with the proposed control strategy. As mentioned in 3.4, the target application is 1.6kW home air-conditioner outdoor unit. The power stage and the control circuit are implemented based on Fig. 3.1 and Fig. 3.9. Specification of all elements is arranged in Table 4.1

Table 4.1 Specification of all elements used in simulation and experiment

Maximum Load Power (P_{Load})	1.6 kW
Grid Voltage (v_{in})	220 Vrms /60 Hz
APF Inductor (L)	1 mH
APF Capacitor (C)	800 μF
DC-link Voltage (V_o)	400 Vdc
Load Inductor (L_{load})	2 mH
Load Capacitor (C_{load})	600 μF
Switching Frequency (f_s)	60 kHz

4.2 Simulation Results

4.2.1 Steady-state Operation

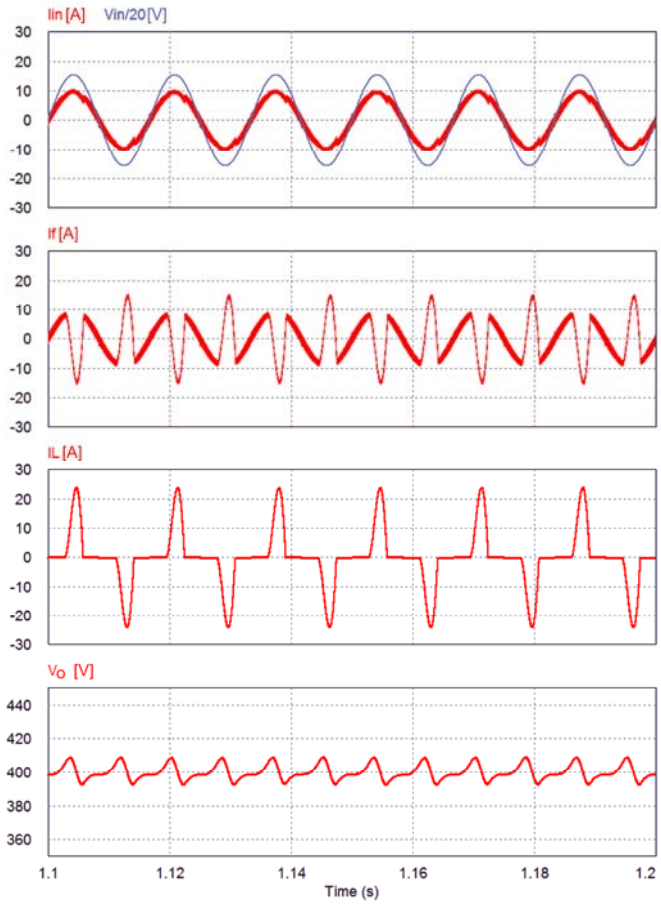

Fig. 4.1 Simulation waveforms of operation under full-load condition.

Fig. 4.1 shows the simulation waveforms of the shunt APF under full-load condition. The dc-link voltage is regulated 400V and the APF current is properly controlled so that the line current has the same shape of the grid voltage and be in phase with it.

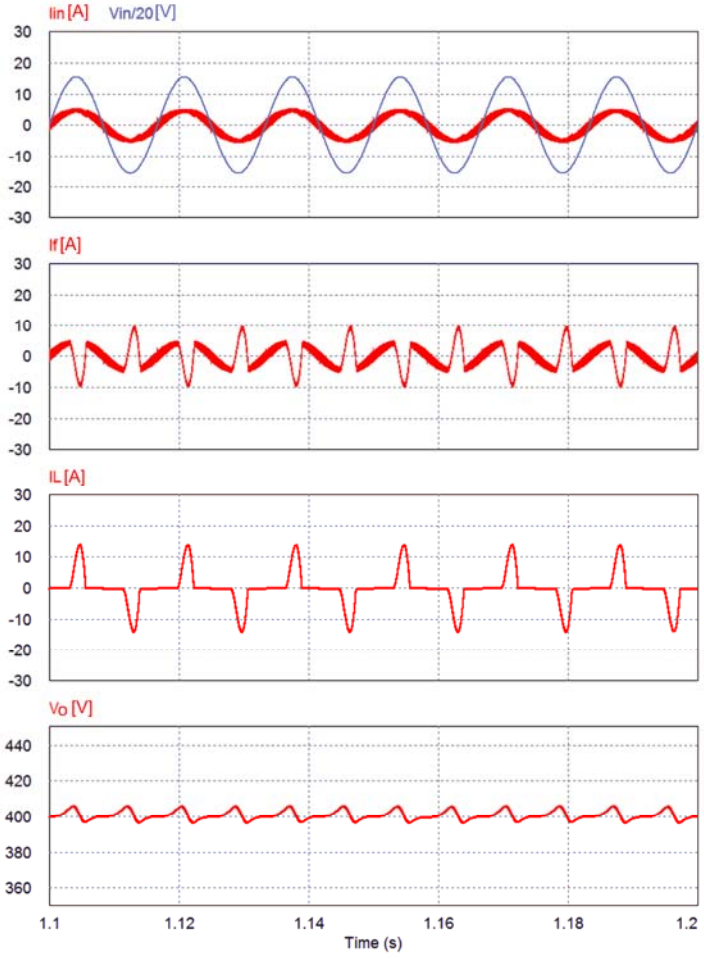

Fig. 4.2 Simulation waveforms of operation under half-load condition.

Fig. 4.2 shows the simulation waveforms of the shunt APF under half-load condition. Alike the full-load condition, dc-link voltage is well regulated and the line current has a sinusoidal shape.

As expected, in both cases, the harmonic and reactive currents are well compensated and the dc-offset problem does not exist due to the applied new control method.

The current loop operation waveforms of the proposed control method are illustrated in Fig. 4.3. The modulated carrier signal is compared to the sensed line current, and the comparator outputs high when the sensed line current reaches the carrier signal. The digital signal processor detects the moment and generates the doubled on-time duty.

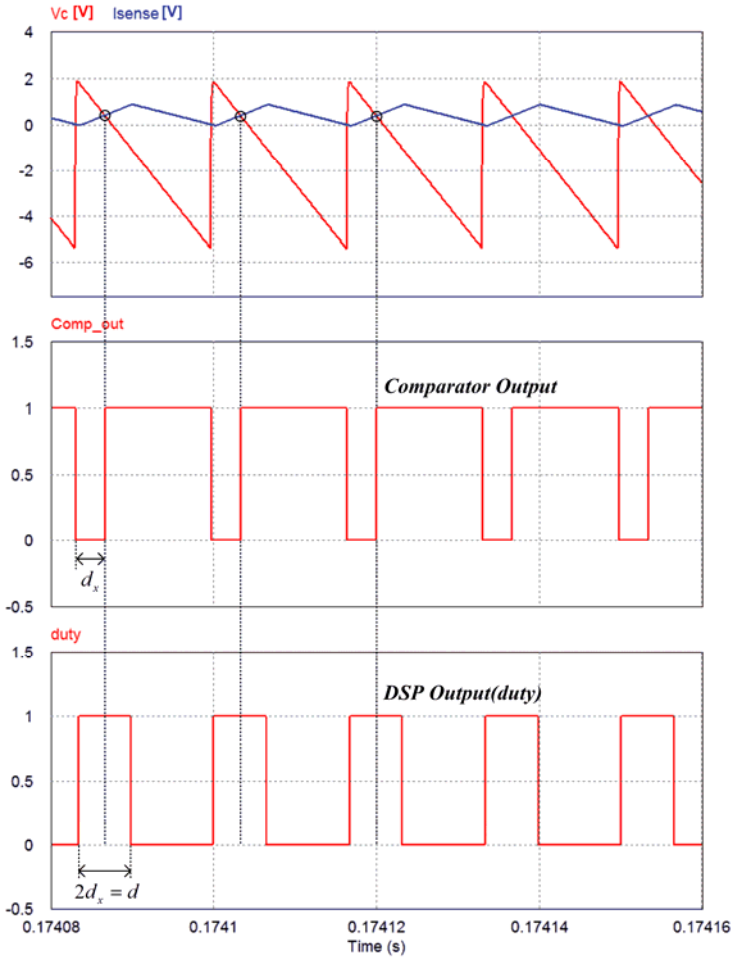

Fig. 4.3 Operation waveforms of the proposed control method.

4.2.2 Load Transient Operation

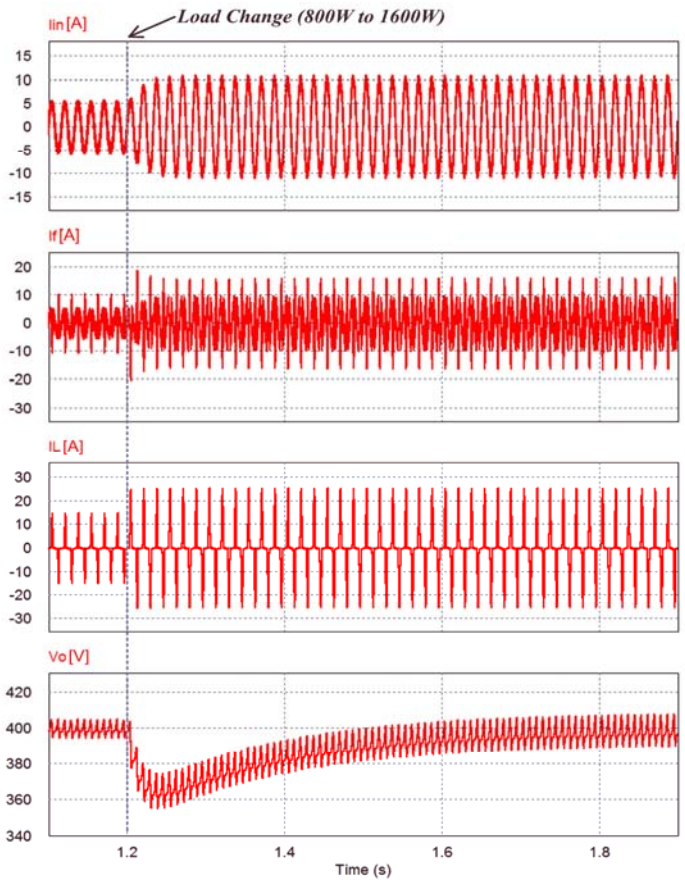

Fig. 4.4 Simulation waveforms of the shunt APF system in transient.

The simulation result of the transient response is shown in Fig. 4.4. At t=1.2s, the load changes from half (800 W) to full (1600 W) condition. Even though the step change in the nonlinear load takes place, the APF with the proposed control method works appropriately. However, the response of the dc-link voltage is slow because of the low bandwidth of the closed voltage loop to prevent the line current from being distorted.

4.3 Experimental Results

4.3.1 Steady-state Operation

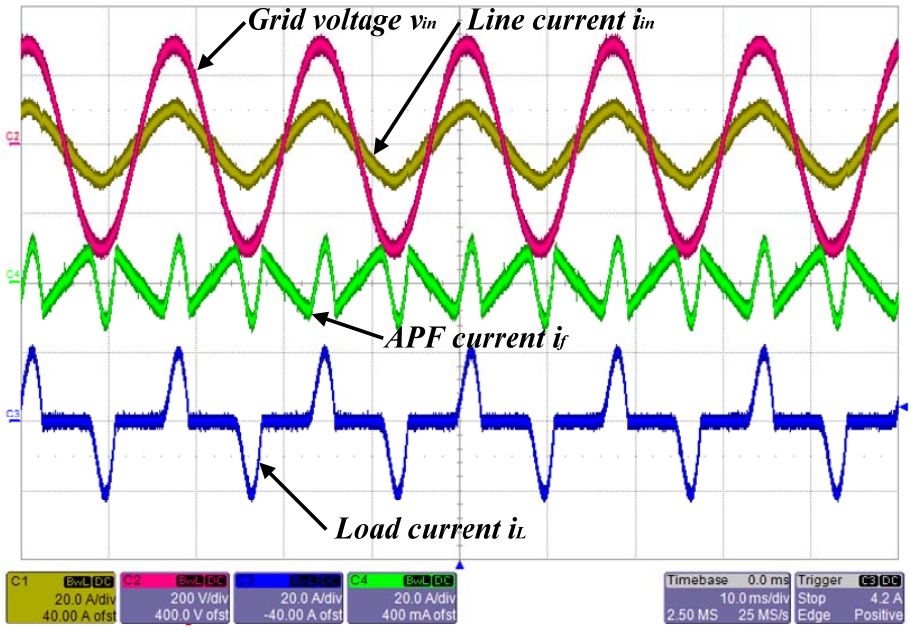

Fig. 4.5 Measured grid voltage, line current, APF current and load current waveforms of the shunt APF system based on the proposed control method at full load condition (v_{in}: 200 V/div, i_{in}:20 A/div, i_f: 20 A/div, i_L: 20 A/div).

Experimental waveforms of the shunt APF system with the proposed control method are shown in Fig. 4.5 and Fig. 4.6. Fig. 4.5 illustrates the grid voltage and the line current at 220-Vrms under full-load condition (1.6-kW nonlinear load), whereas Fig. 4.6 shows them under half-load condition (800-W nonlinear load). It can be seen that the line current is almost sinusoidal and in phase with the grid voltage. These figure show that the dc-offset problem totally disappears both under full and half load conditions due to the inherent

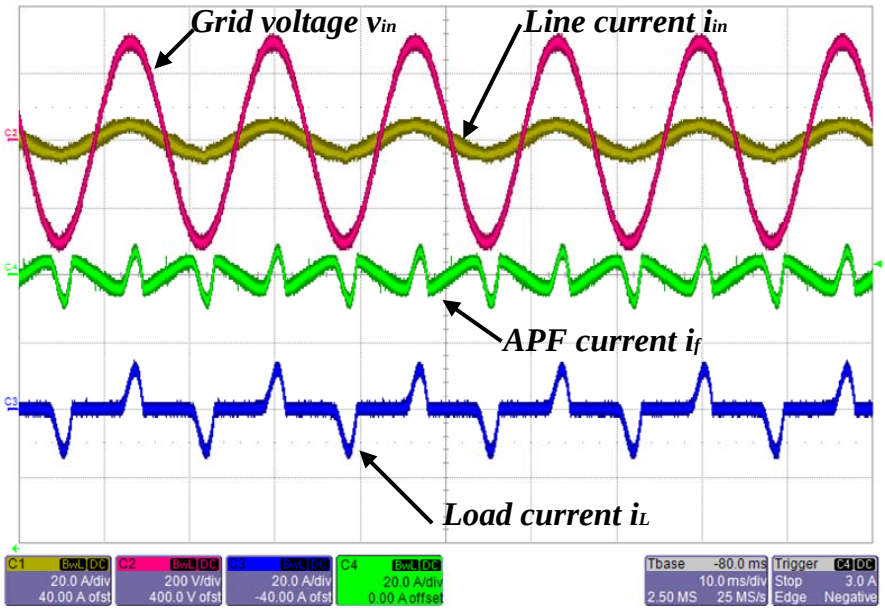

Fig. 4.6 Measured grid voltage, line current, APF current and load current waveforms of the shunt APF system based on the proposed control method at half load condition (v_{in}: 200 V/div, i_{in}:20 A/div, i_f: 20 A/div, i_L: 20 A/div).

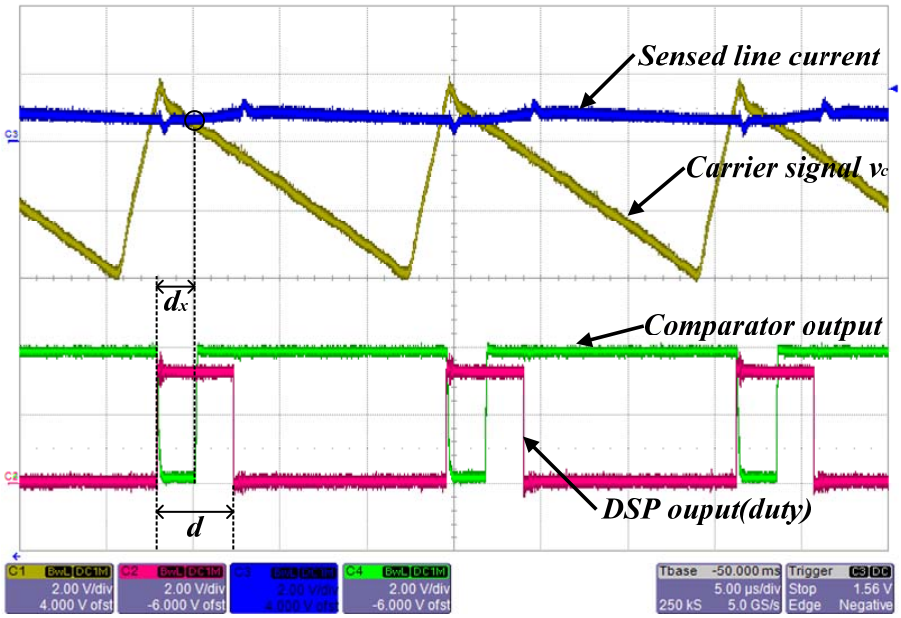

Fig. 4.7 Current control switching mechanism.

characteristic of the proposed control. However, when the load current changes stiffly from peak to zero, the line current is slightly distorted. In 3.3.2, the switching frequency is assumed to be significantly higher than that of line and load so that the load and the APF currents are constant in a switching cycle. Because these current vary slightly in real situation, the line current cannot follow the grid voltage perfectly at the moment the load current drastically changes. If the load current changes slowly in a line cycle, this phenomenon is not observed.

Fig. 4.7 represents the experimental waveforms of current control mechanism. When the sensed line current reaches the carrier signal, comparator outputs a high signal and duty is generated as two-fold of d_x. This allows the average line current to be compared with the carrier signal as intended.

4.3.2 Load Transient Operation

The Experimental result of load transient response is given in Fig. 4.8. The load conditions change from half (800W) to full (1.6kW). As soon as the load increases, the dc-link voltage drops because the amount of harmonic and reactive components abruptly increases and the APF current is not enough to fill the dc-link capacitor in a moment. But the dc-link voltage is raised to the origin right away, 0.4 sec. in this system, which suggests that the voltage compensator is appropriately designed.

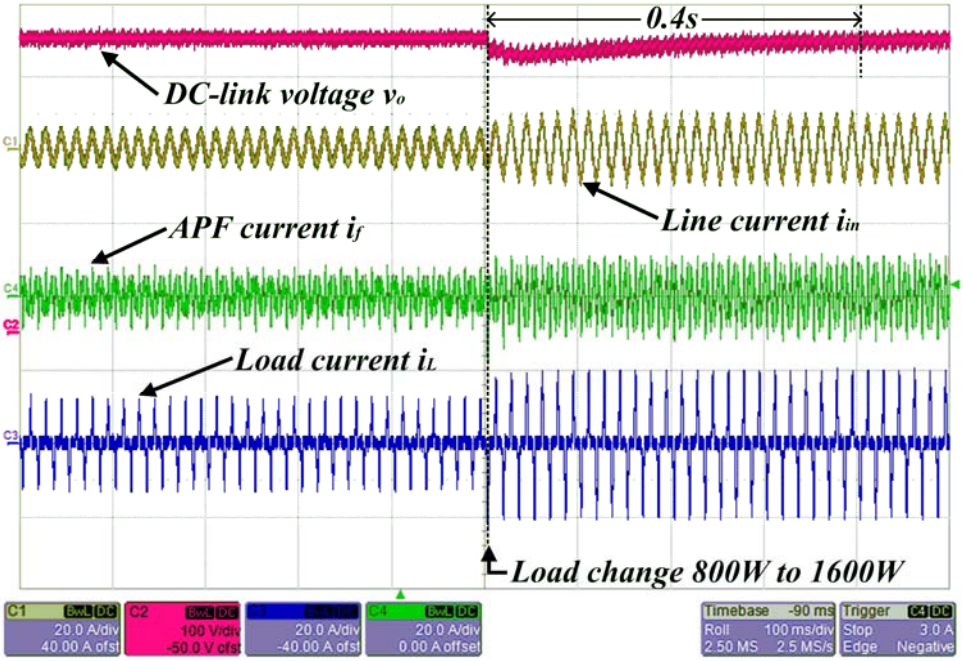

Fig. 4.8 Measured grid voltage, line current, APF current and load current waveforms of the shunt APF system in load transient from 800 W to 1600 W (v_o: 100 V/div, i_{in}:20 A/div, i_f: 20 A/div, i_L: 20 A/div).

Fig. 4.8 validates that the shunt APF system with the described modulated carrier control guarantees magnificent performance not only in steady-state but also in transient-state.

4.3.3 Analysis of Experimental Results

Fig. 4.9 shows the measured power factor of the shunt APF system with the proposed control method at various load conditions. Also, power factor of the nonlinear load system without the shunt APF is represented together. It is noteworthy mentioning that although the system does not include an input filter for switching ripple attenuation, power factor is considerably high.

Further improvement of power factor is expected when the input filter is added to the system.

Lastly, harmonic elements of the line current with and without the APF under full-load (1.6kW) condition at 220-Vrms grid voltage are organized in Fig. 4.10. It is confirmed the system satisfies IEC 61000-3-2 class A with adequate margins. Data in both Fig. 4.9 and Fig. 4.10 are collected by PM-6000 power analyzer.

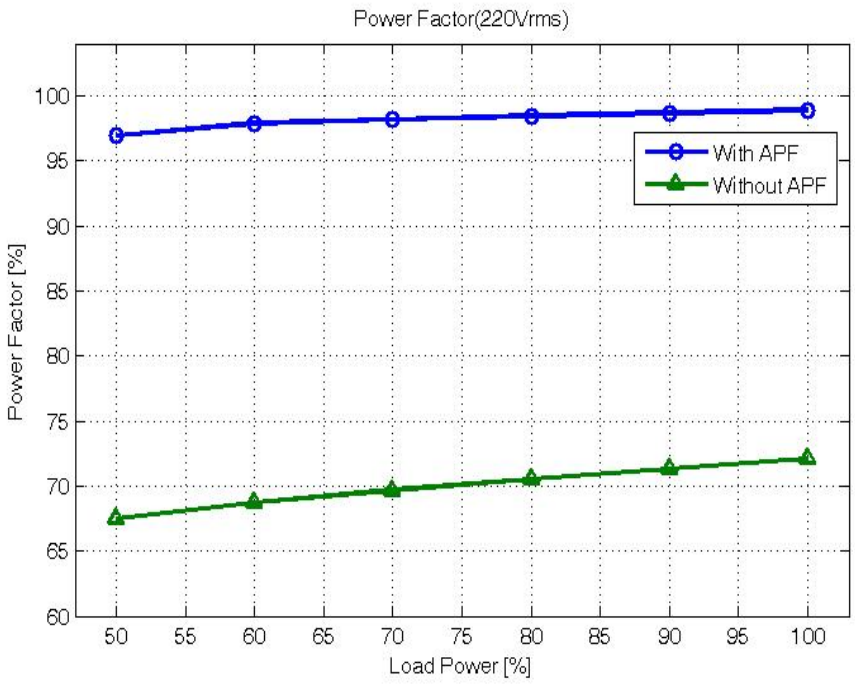

Fig. 4.9 Power factors of the nonlinear load system with and without APF under various load conditions.

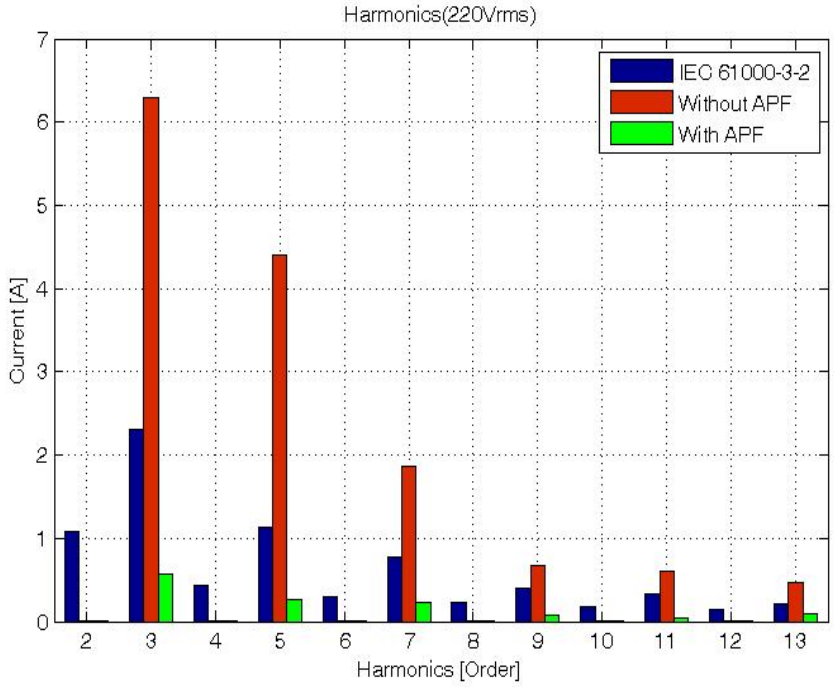

Fig. 4.10 Harmonic elements of the line current with and without the APF under full load (1.6kW) condition.

4.4 Summary

In this chapter, simulation and experimental results verified the performance of the shunt APF system with the proposed modulated carrier control. The simulation results validate the concept of the new control, and 1.6-kW prototype of the single-phase shunt APF system was implemented.

From the experimental results in Fig. 4.5 to Fig. 4.8, regardless of how much currents flow to the nonlinear load, the line current contains mostly the fundamental element. In addition, the proposed shunt APF compensates harmonic and reactive currents without the dc-offset as claimed.

Consequently, the measured harmonic components by PM-6000 comply with the harmonic regulation (IEC 61000-3-2 Class A) on the target application.

5. Conclusion and Future Works

An improved modulated carrier control for single-phase active power filter has been proposed in this thesis. The control method fulfills harmonic and reactive current elimination and gets rid of the dc-offset problem by comparing the carrier signal to the average line current and having the duty ratio doubled.

Prior to the introduction of the new control method, overall harmonic and reactive elimination techniques were reviewed. In addition, pros and cons of previously proposed single-phase shunt active power filter control strategies are analyzed.

Next, the operation principle of the shunt APF is discussed in detail and the control scheme was proven to be plausible theoretically. The new method accepts the control concept of active power factor correction and the current loop mechanism definitely satisfies the concept.

Finally, the simulation and experimental results verify the performance of the proposed control method. A 1.6-kW single-phase shunt active power filter system prototype is implemented and confirms great current compensation capability.

Future work of the thesis is to extend the idea to three-phase systems for larger scale power systems. Since three-phase shunt active power filter normally use six-switches as the control converter, operation principle is different from that of the single-phase system. Also, stability analysis needed for stable operation in wide range of load conditions.

References

[1] A. Mansoor, W. M. Grady, A. H. Chowdhury, and M. J. Samotyi "An investigation of harmonic attenuation and diversity among distributed single-phase power electronic loads," *IEEE Transaction on Power Delivery*, vol. 10, no.15, pp. 467-473, Jan. 1995.

[2] Annabelle V. Zyl, Johan H. R. Enslin, and Rene Spee, "A new unified approach to power quality management," *IEEE Transaction on Power Electronics*, vol. 11, no. 5, pp. 691-697, Sep. 1996.

[3] Mauricio Aredes, Jurgen Hafner, and Klemens Heumann, "Three-phase four-wire shunt active filter control strategies," *IEEE Transaction on Power Electronics*, vol. 12, no. 2, pp. 311-1997, Mar. 1997.

[4] H. Akagi, Y. Kanazawa, and A. Nabae, "Instantaneous reactive power conpensators comprising switching devices without energy storage components," *IEEE Transaction on Industry Applications*, vol. 20, no. 3, pp. 625-630, May/Jun. 1984.

[5] H.-L. Jou, J.-C. Wu, and H.-Y. Chu, "New single-phase active power filter,"*IEE Proc. Electric Power Applications*, May 1994, pp. 129-134.

[6] C.Y. Hsu, and H.Y. Wu, "A new single-phase active power filter with reduced energy-storage capacity," *IEE Pro. Electric Power Applications*, Jan. 1996, pp. 25-30.

[7] Luowei Zhou, and Zecheng Li, "A novel active power filter based on the least compensation current control method," *IEEE Transaction on Power Electronics*, vol. 15, no. 4, pp. 655-659, July 2000.

[8] Hasan Komurcugil, and Osman Kukrer, "A new control strategy for single-

phase shunt active power filters using a Lyapunov function," *IEEE Transaction on Industrial Electronics*, vol. 53, no. 1, pp. 305-312, Feb. 2006.

[9] David A. Torrey, Adel M. A. M., and Al-Zamel, "Single-phase active power filters for multiple nonlinear loads,"*IEEE Transaction on Power Electronics*, vol. 10, no. 3, pp. 263-272, May 1995 .

[10] J.-C. Wu, and H.-L. Jou, "Simplified control method for the single-phase active power filter,"*IEE Proc. Electric Power Applications*, May 1996, pp. 219-224.

[11] Fabiana Pottker, and Ivo Barbi, "Power factor correction of non-linear loads employing a single phase active power filter: control strategy, design methodology and experimentation," PESC'97 Record. 28th annual *IEEE Power electronics Specialists Conference*, 1997, vol.1 pp.412-417.

[12] B. N. Singh, "Sliding mode control technique for indirect current controlled active filter," in *Proc. IEEE Region5 Annual Technical Conference*, 2003, pp. 51-58.

[13] Paolo Mattavelli, and Fernando Pinhabel Marafao, "Repetitive-based control for selective harmonic compensation in active power filters," *IEEE Transaction on Industrial Electronics*, vol. 51, no. 5, pp. 1018-1024, Oct. 2004.

[14] J. Miret, M. Castilla, J. Matas, and J.M. Guerrero "Selective harmonic-compensation control for single-phase active power filter with high harmonic rejection," *IEEE Transaction on Industrial Electronics*, vol. 56, no. 8, pp. 3117-3127, Aug. 2009.

[15] Luowei Zhou, and Keyue M. Smedley, "Unified constant-frequency integration control of active power filter," in *Proc. APEC* , 2000, pp. 406-412.

[16] Keyue M. Smedley, Luowei Zhou, and Chongming Qiao, "Unified constant-

frequency integration control of active power filters-steady-stage and dynamics," *IEEE Transaction on Power Electronics*, vol. 16, no. 3, pp. 428-436, Jul. 2001.

[17] Chongming Qiao, Keyue M. Smedley, and Franco Maddaleno, "A single-phase active power filter with one-cycle control under unipolar operation," *IEEE Transaction on Circuits and Systems*, vol. 51, no. 8, pp. 1623-1630, Aug 2004.

[18] Chongming Qiao, Taotao Jin, and Smedley K.M. "One-cycle control of three-phase active power filter with vector operation," *IEEE Transaction on Industrial Electronics*, vol. 51, no. 2, pp. 455-463, Apr. 2004 .

[19] Sreeraj E. S., Prejith E. K., Chatterjee K., and Bandyopadhyay S., "An active harmonic filter based on one cycle control," *IEEE Transaction on Industrial Electronics*, Early access article, 2013.

[20] Elham B. Makram, E.V. Subramaniam, Adly A. Girgis, and Ray Catoe, "Harmonic filter design using actual recorded data," *IEEE Transaction on Industrial Application*, vol. 29, no. 6, pp. 1176-1183, Nov. 1993.

[21] Fakhralden A. Huliehel, Fred C. Lee, and Bo H. Cho, "Small-signal modeling of the single-phase boost high power factor converter with constant frequency control," PESC'92 Record. 23rd annual *IEEE Power electronics Specialists Conference*, 1992, vol.1 pp.475-482.

[22] Akagi, H. "Trends in active power line conditioners," *IEEE Transaction on Power Electronics*, vol. 9, no. 3, pp. 263-268, May 1994.

[23] Raymond B. Ridley, "A new, continuous-time model for current-mode control,", *IEEE Transaction on Power Electronics*, vol. 6, no. 2, pp. 271-280, Apr. 1991.

[24] Wei Tang, Fred C. Lee, and Raymond B. Ridley, "Small-signal modeling of

average current-mode control," *IEEE Transaction on Power Electronics*, vol. 8, no. 2, pp. 112-119, Apr. 1993.

[25] Wei Tang, Fred C. Lee, Raymond B. Ridley, and Isaac Cohen, "Charge control: modeling, analysis, and design," *IEEE Transaction on Power Electronics*, vol. 8, no. 4, pp. 396-403, Apr. 1993.

[26] Dragan Maksimovic, Yungtaek Jang, and Robert W. Erickson, "Nonlinear-carrier control for high-power-factor boost rectifiers," *IEEE Transaction on Power Electronics*, vol. 11, no. 4, pp. 578-584, Jul. 1996.

[27] Williams, J. B, "Design of feedback loop in unity power factor AC to DC converter," PESC'89 Record. 20th annual *IEEE Power electronics Specialists Conference*, 1989, vol.2 pp.959-967.

[28] R.B. Ridley, "Average small-signal analysis of the boost power factor correction circuit," VPEC Seminar Proceedings, 1989, pp. 108-120.

[29] Peng, F. Z., "Harmonic sources and filtering approaches," *IEEE Transaction on Industrial Application Magazine*, vol. 7, no. 4, pp. 18-25, Jul. 2001.

[30] Smedley K. M., and Cuk Slobodan, "One-cycle control of switching converters," PESC'91 Record. 22nd annual *IEEE Power electronics Specialists Conference*, 1991, pp.888-896.

[31] Teodorescu R., Blaabjerg F., Liserre M., and Loh P.C., "Proportional-resonant controllers and filters for grid-connected voltage-source converters," *IEE Pro. Electric Power Applications*, Sep. 2006, pp. 750-762.

[32] Zmood D.N., and Holmes D.G, "Stationary frame current regulation of PWM inverters with zero steady state error," *IEEE Transaction on Power Electronics*, vol. 18, no. 3, pp. 814-822, Apr. 2003.

[33] Hye-Jin Kim, Bo-Hyung Cho, and Hangseok Choi, "Interleaved continuous

conduction mode power factor correction boost converter with improved modulated carrier control method," in *Proc. APEC* , 2013, pp. 351-355.

[34] H. Choi, "Continuous conduction mode power factor correction circuit with reduced sensing requirement", U.S. patent US8,279,630, Oct. 2012

[35] Peng. F.Z., "Harmonic source and filtering approaches," *IEEE Transaction on Industry Application Magazine*, vol. 7, no. 4, pp. 18-25, Jul./Aug. 2001.

국문 초록

본 논문은 향상된 변조 반송파 신호(improved modulated carrier signal)를 이용하여 비선형 부하로부터 발생하는 입력 전원의 고조파 및 무효 성분 전류를 제거하는 단상 능동 전력 필터의 새로운 제어 기법을 제안한다.

새로이 제안되는 제어 기법은 입력 전류의 평균값과 변조 반송파 신호를 비교한 후, 시비율 (duty)을 두 배로 만들어 줌으로써 입력 전류가 입력 전압과 동상이 되고 정현파(sinusoidal)의 형태를 가지도록 직접 입력 전류를 제어한다. 반송파 신호와 비교되는 입력 전류의 값이 최대값이 아닌 평균값이기 때문에, 기존의 유사한 제어 방식들에서 발생하는 직류오프셋 (dc-offset) 이슈가 효과적으로 처리된다. 결과적으로, 본 논문에서 제안된 제어 기법은 고조파 및 무효 전류 성분을 적절히 제거하고 직류오프셋 문제를 해결한다.

본 논문에서는 제안된 제어 기법을 이용한 능동 전력 필터의 동작을 자세하게 분석하고, 설계 가이드라인을 제시한다. 프로토타입(prototype) 하드웨어를 기반으로 한 실험 결과를 통하여 제안된 제어 기법을 이용한 단상 능동 전력 필터의 성능을 검증한다.

주요어: 비선형 부하, 병렬 능동 전력 필터, 고조파 및 무효 성분 전류 보상, 향상된 변조 반송파 제어.

학 번: 2012-20794

감사의 글

2년 전, 대학원 생활에 첫발을 내딛던 순간이 기억납니다. 큰 꿈과 기대감, 그리고 막연한 두려움이 공존했던 가슴 떨리는 순간이었습니다. 잘 해낼 수 있다는 자신감이 있었고, 많이 배우겠다는 각오가 있었으며, 더 하려야 더 할게 없는 최선의 노력을 다하겠노라 하는 결의가 있었습니다. 그렇게 시작한 대학원 생활을 이제 마무리 할 시간이 왔습니다. 2년간의 시간을 정리하며 이 글을 빌어 많은 분들께 감사 드리고 싶습니다.

먼저 2년 동안 저를 지도해주시고 인생의 지침을 제시해주신 저의 지도교수님, 조보형 교수님께 감사 드립니다. 어떤 마음 가짐으로 삶을 대해야 하는가를 생각하게 해주시고 일깨워주신 교수님의 가르침을 잊지 않겠습니다. 항상 강조하셨던 스스로 문제를 제기하고 해결하는 능력, 통찰력을 가지라고 하셨던 말씀, 가슴 깊은 곳에 품고 사회로 나가 훌륭한 엔지니어가 되도록 노력하겠습니다. 그리고 제 진로에 대해 세심하게 신경 써주시고 관심 가져 주셨던 설승기 교수님, 프로젝트를 수행할 때 많은 조언과 도움을 주신 하정익 교수님께도 감사의 말씀을 전합니다.

더불어 석사 과정 동안 저의 보금자리였던 서울대학교 301동 617호 PESL 식구들. 선배님, 동기들, 후배들과 함께한 시간을 평생 잊지 못할 것입니다. 하늘 같은 선배이시면서도 온화한 미소로 항상 조언해주시고 도움을 주셨던 정원이형, 미국에서 열심히 연구 중인 종원이형, 부드러운 리더십과 따뜻한 마음으로 챙겨주신 종복이형, 힘들었던 프로젝트를 무사히 잘 마칠 수 있도록 이끌어준 규식이형, 대학원 생활의 정석을 보여준

갑수형, 친구이지만 한참 선배인 성격 좋은 승운이, 묵묵히 많은 일을 수행하면서도 특유의 꼼꼼함을 가진 창윤이형께 진심으로 감사 드립니다. 많은 도움을 받았고, 힘들 때 의지 할 수 있었으며, 최고의 선배이자 친구였던 김혜진, 사회에 나가 열심히 일하고 있는 철우형, 재즈가 무엇인지 음악의 소중함이 무엇인지 알게 해주고 삶에 대해 깊이 고찰을 할 수 있도록 해준 장바울, 소울을 공유한 나의 소중한 브라더 최우인, 진짜 근성이 무엇인지 보여준 이제현에게 감사의 마음을 전하고 싶습니다. 이제 험난한 석사 2년차의 길로 접어드는 후배들 상우, 성현이게도 무궁한 발전이 있기를 바라며, 곧 사회로 첫발을 내딛는, 2년 동안 동고동락했던 동기들 두호, 준혁이에게 앞으로 찬란한 미래가 다가오기를 기원합니다. 그리고 마지막까지 관심 가지고 프로젝트를 잘 마무리 할 수 있도록 도와주신 승준이형과 설방, 하방 분들께도 감사 드립니다.

힘든 시기에 곁에 있어주고, 응원해주며, 세상에서 가장 아름다운 미소로 저에게 힘이 되어준 하늬에게 사랑하고 감사하다고 전하고 싶습니다.

마지막으로 저를 사랑과 정성으로 키워주신 부모님. 정말 정말 사랑하고 감사 드립니다. 두 분이 몸소 보여주신 바른 생활, 굳은 의지, 긍정적인 마음가짐, 삶에 대한 성실한 태도가 제 마음 속 깊은 곳에 자리잡고 있었기에 이 모든 일을 할 수 있었습니다. 두 분의 아들이라는 것에 항상 감사하며 자랑스럽습니다. 그리고 하나뿐인 나의 동생 기서. 우리 가족 사랑합니다.

감사합니다.

2014년 2월
손기봉